

JAERI - M

86-124

PROF-DD

A CODE SYSTEM FOR GENERATION OF
MULTI-GROUP DOUBLE-DIFFERENTIAL FORM
CROSS SECTION LIBRARY

August 1986

Takamasa MORI, Masayuki NAKAGAWA and Yukio ISHIGURO

日本原子力研究所
Japan Atomic Energy Research Institute

JAERI-M レポートは、日本原子力研究所が不定期に公刊している研究報告書です。
入手の問合せは、日本原子力研究所技術情報部情報資料課（〒319-11 茨城県那珂郡東海村）
あて、お申しこしください。なお、このほかに財団法人原子力弘済会資料センター（〒319-11 茨城
県那珂郡東海村日本原子力研究所内）で複写による実費頒布をおこなっております。

JAERI-M reports are issued irregularly.

Inquiries about availability of the reports should be addressed to Information Division, Department
of Technical Information, Japan Atomic Energy Research Institute, Tokai-mura, Naka-gun,
Ibaraki-ken 319-11, Japan.

© Japan Atomic Energy Research Institute, 1986

編集兼発行 日本原子力研究所
印 刷 山田軽印刷所

PROF-DD

A Code System for Generation of Multi-Group
Double-Differential Form Cross Section Library

Takamasa MORI, Masayuki NAKAGAWA and Yukio ISHIGURO

Department of Reactor Engineering

Tokai Research Establishment

Japan Atomic Energy Research Institute

Tokai-mura, Naka-gun, Ibaraki-ken

(Received July 28, 1986)

The PROF-DD code system has been developed to generate the multi-group double-differential form cross section (DDX) library by processing the nuclear data file compiled with the ENDF/B-IV or -V format. This system consists of five steps : MCFILEF, RESENDD, SPINPTF, PROF-DDX and DDXLIBMK. By using this system, a user can easily produce a multi-group DDX library with a few input data, and make figures of the processed DDX data. The produced DDX library can be used for fusion neutronic calculations by the Monte Carlo code MORSE-DD, 1- and 2-dimensional Sn transport codes ANISN-DD and DOT-DD. This report has been prepared as a user manual of the PROF-DD code system.

Keywords: Multi-Group Double-Differential Form Cross Section, Fusion Neutronics, Transport Calculation, Code System, DDX Library, ENDF/B Format, Manual

P R O F - D D

多群二重微分型断面積ライブラリー作成コードシステム

日本原子力研究所東海研究所原子炉工学部

森 貴正・中川正幸・石黒幸雄

(1986年7月28日受理)

ENDF/B-IVあるいは-V形式の評価済み核データファイルを処理して、多群二重微分型断面積(DDX)ライブラリーを作成するコードシステムPROF-DDを開発した。本コードシステムは、MCFILEF, RESEND, SPINPTF, PROF-DDX及びDDXLIBMKの5ステップから構成されている。本コードシステムを使用することにより簡単に多群DDXライブラリーを作成することができる。また作図による比較も行うことができる。作成されたライブラリーは、モンテカルロコードMORSE-DD, 一次元及び二次元SnコードANISN-DDとDOT-DDを用いることにより核融合炉ニュートロニクス解析に使用することができる。本報は、PROF-DDコードシステムのユーザーマニュアルとして作成された。

Contents

1. Introduction	1
2. Multi-Group Double-Differential Form Cross Section	2
2.1 Definition of Duble-Differential Form Cross Section	2
2.2 Calculation of Multi-Group Double-Differential Form Cross Section	3
3. Multi-Group DDX Library Generation Code System :	
PROF-DD	7
3.1 General Feature of PROF-DD	7
3.2 MCFILEF	8
3.2.1 Input Instruction	9
3.2.2 Sample Input, JCL and I/O Files	11
3.3 RESENDD	11
3.3.1 Input Instruction for the PROF-DD System	12
3.3.2 Sample Input, JCL and I/O Files	12
3.4 SPINPTF	13
3.4.1 Input Instruction	13
3.4.2 Sample Input, JCL and I/O Files	14
3.5 PROF-DDX	14
3.5.1 Outline of PROF-DDX	14
3.5.2 Input Instruction	19
3.5.3 Sample Input, JCL and I/O Files	20
3.6 DDXLIBMK	20
3.6.1 Input Instruction	20
3.6.2 Sample Input, JCL and I/O Files	21
3.6.3 Structure of DDX Library	22
4. Auxiliary Programs	33
4.1 DDXPLOT	33
4.2 Dump of DDX Data In Master File	36
5. Concluding Remarks	48
Acknowledgments	48
References	49
Appendix Available DDX Libraries	
A.1 DDXLIB1 and DDXLIB3 Libraries	50
A.2 Comparison between DDXLIB1 and DDXLIB3 Libraries ..	51

目 次

1. 序	1
2. 多群二重微分型断面積	2
2.1 二重微分型断面積の定義	2
2.2 多群二重微分型断面積の計算	3
3. 多群DDXライブラリー作成コードシステム：PROF-DD	7
3.1 PROF-DDの概要	7
3.2 MCFILEF	8
3.2.1 データ入力の方法	9
3.2.2 入力データ, JCLの例とI/Oファイル	11
3.3 RESENDD	11
3.3.1 PROF-DDシステムでのデータ入力	12
3.3.2 入力データ, JCLの例とI/Oファイル	12
3.4 SPINPTF	13
3.4.1 データ入力の方法	13
3.4.2 入力データ, JCLの例とI/Oファイル	14
3.5 PROF-DDX	14
3.5.1 PROF-DDXの概要	14
3.5.2 データ入力の方法	19
3.5.3 入力データ, JCLの例とI/Oファイル	20
3.6 DDXLIBMK	20
3.6.1 データ入力の方法	20
3.6.2 入力データ, JCLの例とI/Oファイル	21
3.6.3 DDXライブラリーの構成	22
4. 補助プログラム	33
4.1 DDXPLOT	33
4.2 マスターファイルのダンプ	36
5. 結び	48
謝辞	48
参考文献	49
付録 DDXライブラリー	50
A. 1 DDXLIB1とDDXLIB3ライブラリー	50
A. 2 DDXLIB1とDDXLIB3の比較	51

1. Introduction

The anisotropy of neutron scattering angular distribution plays an important role in the neutron energy and spatial distributions at the high energy region as encountered in fusion reactor shielding and blanket neutronics calculations. The conventional multi-group method using the P_1 expansion for anisotropic scattering sometimes significantly mispredicts the neutron transport phenomena in the materials with highly anisotropic scattering cross sections. The use of the lower order P_1 expansion of the angular distribution leads to negative energy transfer matrices, hence sometimes to negative flux. Moreover, the conventional multi-group method can not accurately take account of the energy-angle correlated kinematics for neutron scattering. In order to overcome such problems, the use of the double-differential form of scattering cross sections(DDX) was proposed for the accurate treatment of the energy-angle correlated kinematics by Takahashi *et al.*¹⁾. The transport codes using this type of cross section can treat accurately the strongly anisotropic scattering observed in the fusion blanket and shielding materials.

At the present work, the PROF-DD code system has been developed to produce the multi-group DDX library by processing the nuclear data file compiled with the ENDF/B-IV or -V format. This system consists of five steps corresponding to five independent codes : MCFILEF, RESENDD, SPINPTF, PROF-DDX and DDXLIBMK. The PROF-DDX code is a main code of this system, which calculates the multi-group DDX and saves them on a master PDS file. The MCFILEF code generates a control file for the PROF-DDX code which contains energy group and angle bin structures. The SPINPTF code prepares an input data file for the PROF-DDX code by combining the control file and other input data. The DDXLIBMK code edits a DDX library for transport calculations from the master PDS file. The resonance cross section calculation and Doppler broadening calculation are performed by the RESENDD code.

The validation tests of the produced DDX library have been carried out by the MORSE-DD code²⁾ and reported elsewhere³⁾. The DDX library can be used by other 1- and

2-dimensional Sn transport codes ANISN-DD and DOT-DD⁴⁾.

This report has been prepared as a user manual of the PROF-DD code system. The description for an auxiliary program DDXPLOT is also given. By using this system, a user can easily produce a multi-group DDX library and plot the results by the DDXPLOT code. In Appendix, the newly produced DDX library DDXLIB3 and some results of benchmark calculations with use of this library are presented.

2. Multi-Group Double-Differential Form Cross Section

2.1 Definition of Double-Differential Form Cross Section

The collision source term in the transport equation is written as

$$\begin{aligned} q(r, \Omega, E) = & \int dE' \int d\Omega' \phi(r, \Omega', E') \sum_j N_j \{ \sigma_{el}^j(\Omega' \rightarrow \Omega, E' \rightarrow E) \\ & + \sum_i \sigma_{in,i}^j(\Omega' \rightarrow \Omega, E' \rightarrow E) + \sum_m m \sigma_{n,mn}^j(\Omega' \rightarrow \Omega, E' \rightarrow E) \\ & + \sum_X \sigma_{n,n'X}^j(\Omega' \rightarrow \Omega, E' \rightarrow E) \}. \end{aligned} \quad (1)$$

where σ^j denotes the microscopic differential cross section of nuclide j , and the subscript el stands for elastic scattering, (in, i) discrete and continuum level inelastic scattering, (n, mn) neutron multiplying reaction emitting m neutrons, ($n, n'X$) neutron and charged particle emission. If we define the production cross section by

$$\sigma_{pr}(E) = \sigma_{el}(E) + \sum_i \sigma_{in,i}(E) + \sum_m m \sigma_{n,mn}(E) + \sum_X \sigma_{n,n'X}(E). \quad (2)$$

Equation (1) can be written as

$$\begin{aligned} q(r, \Omega, E) = & \int dE' \int d\Omega' \phi(r, \Omega', E') \\ & \times \sum_j N_j \{ \sigma_{pr}^j(E') \sum_x R_x^j(E') P_x^j(\mu, ; E' \rightarrow E) \}, \end{aligned} \quad (3)$$

where

$$\mu = \Omega \cdot \Omega' \quad \text{and} \quad R_x(E') = m_x \sigma_x(E') / \sigma_{pr}(E').$$

$P_x(\mu; E' \rightarrow E)$ is the energy-angle distribution of neutrons emitted from the reaction x . Summation over all reaction types

2-dimensional Sn transport codes ANISN-DD and DOT-DD⁴⁾.

This report has been prepared as a user manual of the PROF-DD code system. The description for an auxiliary program DDXPLOT is also given. By using this system, a user can easily produce a multi-group DDX library and plot the results by the DDXPLOT code. In Appendix, the newly produced DDX library DDXLIB3 and some results of benchmark calculations with use of this library are presented.

2. Multi-Group Double-Differential Form Cross Section

2.1 Definition of Double-Differential Form Cross Section

The collision source term in the transport equation is written as

$$\begin{aligned} q(r, \Omega, E) = & \int dE' \int d\Omega' \varphi(r, \Omega', E') \sum_j N_j \{ \sigma_{el}^j(\Omega' \rightarrow \Omega, E' \rightarrow E) \\ & + \sum_i \sigma_{in,i}^j(\Omega' \rightarrow \Omega, E' \rightarrow E) + \sum_m m \sigma_{n,mn}^j(\Omega' \rightarrow \Omega, E' \rightarrow E) \\ & + \sum_X \sigma_{n,n'X}^j(\Omega' \rightarrow \Omega, E' \rightarrow E) \}. \end{aligned} \quad (1)$$

where σ^j denotes the microscopic differential cross section of nuclide j , and the subscript el stands for elastic scattering, (in, i) discrete and continuum level inelastic scattering, (n, mn) neutron multiplying reaction emitting m neutrons, ($n, n'X$) neutron and charged particle emission. If we define the production cross section by

$$\sigma_{pr}(E) = \sigma_{el}(E) + \sum_i \sigma_{in,i}(E) + \sum_m m \sigma_{n,mn}(E) + \sum_X \sigma_{n,n'X}(E). \quad (2)$$

Equation (1) can be written as

$$\begin{aligned} q(r, \Omega, E) = & \int dE' \int d\Omega' \varphi(r, \Omega', E') \\ & \times \sum_j N_j \{ \sigma_{pr}^j(E') \sum_x R_x^j(E') P_x^j(\mu, ; E' \rightarrow E) \}, \end{aligned} \quad (3)$$

where

$$\mu = \Omega \cdot \Omega' \quad \text{and} \quad R_x(E') = m_x \sigma_x(E') / \sigma_{pr}(E').$$

$P_x(\mu; E' \rightarrow E)$ is the energy-angle distribution of neutrons emitted from the reaction x . Summation over all reaction types

is reduced to the double-differential form cross section

$$\sigma(\mu; E' \rightarrow E) = \sigma_{pr}(E') \sum_x R_x(E') P_x(\mu; E' \rightarrow E) = \sigma_{pr}(E') I(\mu; E' \rightarrow E), \quad (4)$$

where $I(\mu; E' \rightarrow E) = \sum_x R_x(E') P_x(\mu; E' \rightarrow E)$.

The energy-angle distribution function $P_x(\mu; E' \rightarrow E)$ can be written as

$$P_x(\mu; E' \rightarrow E) = g_x(E; E') h_x(\mu; E', E), \quad (5)$$

where $g_x(E; E')$ is an energy distribution of secondary neutron and $h_x(\mu; E', E)$ an angular distribution of this neutron. These functions can be calculated based on the kinematics, if it is known, as follows:

$$g_x(E; E') = \frac{f_x(\mu_c; E')}{2\pi} + \frac{d\mu_c}{dE} = \frac{f_x(\mu_c; E')}{2\pi} \frac{2}{(1-\alpha)E' \beta_x(E')}, \quad (6)$$

$$h_x(\mu; E', E) = \delta(\mu - \mu_x^*) \quad (7)$$

where f_x is an angular distribution in the center of mass (CM) system, and

$$\alpha = \left(\frac{A-1}{A+1}\right)^2, \quad (8)$$

$$\mu_c = \left\{ \frac{(A+1)^2}{2A} \frac{E}{E'} - \frac{A}{2} \beta(E')^2 - \frac{1}{2A} \right\} \frac{1}{\beta_x(E')}, \quad (9)$$

$$\mu_x^* = \frac{A+1}{A} \sqrt{E/E'} - \frac{A-1}{2} \sqrt{E'/E} - \frac{AQ_x}{2\sqrt{EE'}}, \quad (10)$$

$$\beta_x(E') = \sqrt{1 + \frac{A+1}{A} \frac{Q_x}{E'}}. \quad (11)$$

In these equations, A and Q_x are the ratio of the mass of the target atom to that of neutron and the Q -value of reaction x , respectively. When the kinematics are not known, functions g_x and h_x are given in Files 4 and 5 of evaluated data file with ENDF/B format, respectively, or $P_x(\mu; E' \rightarrow E)$ is given explicitly in File 6.

2.2 Calculation of Multi-Group Double-Differential Form Cross Section

The multi-group form of energy-angle distribution of secondary neutrons within the g -th energy group in the k -th

angular interval $P_x(k; g' \rightarrow g)$ is obtained by

$$P_x(k; g' \rightarrow g) = \int_{\Delta g'} dE' \int_{\Delta g} dE \int_{\Delta \mu_k} 2\pi d\mu \sigma_x(E') P_x(\mu; E' \rightarrow E) \Psi_w(E') \\ / \int_{\Delta E_g} \sigma_x(E') \Psi_w(E'), \quad (12)$$

where $\Psi_w(E)$ is a weighting function. When the kinematics for reaction x are known, Eq. (12) can be calculated as follows:

$$P_x(k; g' \rightarrow g) = \frac{1}{\sigma_{xg} \Psi_{wg}} \int_{E_{g'+1}}^{E_g} dE' \int_{E_{g+1}}^{E_g} dE \int_{\mu_{k+1}}^{\mu_k} 2\pi d\mu \sigma_x(E') \frac{f_x(\mu_c; E')}{2\pi} \\ \times \frac{2}{(1-\alpha)E' \beta_x(E')} \delta(\mu - \mu_x^*) \Psi_w(E') \\ = \frac{1}{\sigma_{xg} \Psi_{wg}} \int_{E_{g'+1}}^{E_g} dE' \int_{E_{g+1}}^{E_g} dE \sigma_x(E') f_x(\mu_c; E') \Psi_w(E') \\ \times \frac{2}{(1-\alpha)E' \beta_x(E')} \\ \times [H(\mu_k - \mu_x^*(E', E)) - H(\mu_{k+1} - \mu_x^*(E', E))], \quad (13)$$

where H is the heaviside step function defined by

$$H(x) = \begin{cases} 1, & \text{if } x \geq 0 \\ 0, & \text{if } x < 0. \end{cases}$$

In the PROF-DD system, it is assumed that

$$f_x(\mu_c; E') = f_{xg}(\mu_c) \quad (\text{=constant within } g'-\text{th group.})$$

When $\mu - \mu_x^*(E', E) = 0$,

$$E' = \frac{E}{(A-1)^2} \left(\mu - \sqrt{A^2 - 1 - A(A-1) \frac{Q_x}{E} + \mu^2} \right). \quad (14)$$

This relation is plotted in Fig. 2.1 for some values of μ . The integrand in Eq. (13) has non-zero values in the region between the two curves assigned by $\mu = \mu_k$ and $\mu = \mu_{k+1}$. Therefore the integration with respect to E' and E is carried out in the hatched region in this figure, for instance.

As for the reactions such as continuum inelastic scattering, the integration with respect to E and μ can be carried out separately as follows:

$$P_x(k; g' \rightarrow g) = P_1(k; g') \cdot P_2(g; g'), \quad (15)$$

where

$$P_1(k; g') = \int_{\Delta g'} dE' \int_{\Delta \mu_k} d\mu h_x(\mu; E') \sigma_x(E') \Psi_w(E') / \sigma_{xg} \Psi_{wg}, \quad (16)$$

$$P_2(g; g') = \int_{\Delta E_g} dE' \int_{\Delta E_g} dE g_x(E; E') \sigma_x(E') \Psi_w(E') / \sigma_{xg} \Psi_{wg}. \quad (17)$$

The factor $\sigma_x(E') \Psi_w(E')$ in these two equations is assumed to be constant. Instead of Eq. (15), if required, we can adopt the following probability calculated with additional assumption that no neutron emerges in the direction k from the scattering reaction with higher energy than E_{max}^k , which is determined on the basis of the two-body reaction kinematics. With this assumption, the probability of Eq. (15) is modified as follows:

$$P_x(k; g' \rightarrow g) = 0.0 \quad \text{for all } g \text{ such as } E_{g+1} \geq E_{max}^k,$$

and they are renormalized as

$$\sum_g P_x(k; g' \rightarrow g) = P_1(k; g').$$

If $P_x(\mu; E' \rightarrow E)$ is explicitly given in the evaluated data file (File 6), this probability can be processed as follows: At first,

$$P_x(\mu; g' \rightarrow g) = \int_{\Delta E_g} dE' \int_{\Delta E_g} dE P_x(\mu; E' \rightarrow E) \sigma_x(E') \Psi_w(E') / \sigma_{xg} \Psi_{wg},$$

then

$$P_x(k; g' \rightarrow g) = \int_{\Delta \mu_k} d\mu P_x(\mu; g' \rightarrow g). \quad (15')$$

In the PROF-DD system, the lowest energy group is assumed to be the thermal neutron group. The energy-angle distribution of neutrons scattered into this group is automatically calculated, though several optional procedures are prepared for the calculation of the self-group scattering cross section as mentioned in Chapter 3.

By using $P_x(k; g' \rightarrow g)$, the multi-group DDX is written as

$$\sigma(k; g' \rightarrow g) = \sigma_{pr,g'} I(k; g' \rightarrow g) = \sigma_{pr,g'} \sum_x R_x(g') P_x(k; g' \rightarrow g). \quad (18)$$

Accordingly, the collision term presented in Eq. (1) is rewritten as

$$\begin{aligned} q_g(r, \Omega) &= \sum_{g'} \int d\Omega' \varphi_{g'}(r, \Omega') \sum_j N_j \frac{\sigma^j(k; g' \rightarrow g)}{2\pi \Delta \mu_k}, \\ &= \sum_{g'} \int d\Omega' \varphi_{g'}(r, \Omega') \sum_j N_j \sigma_{pr,g'}^j \frac{I^j(k; g' \rightarrow g)}{2\pi \Delta \mu_k}, \end{aligned} \quad (19)$$

where k indicates an angle bin such as $\mu_{k+1} < \Omega \cdot \Omega' < \mu_k$.

In the Sn transport code, Eq.(19) is calculated as follows:

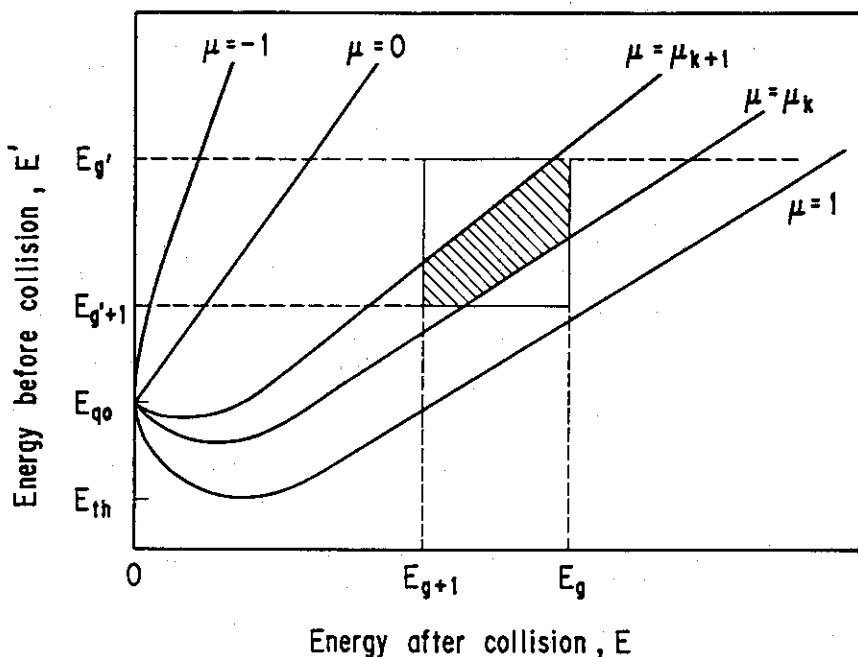
$$q_{g,m} = \sum_{g'} \sum_m \varphi_{g',m} \cdot w_m \cdot \sum_{\mu_k} \left(\sum_j N_j \sigma_{pr,g}^j \frac{I^j(k; g' \rightarrow g)}{2\pi\Delta\mu_k} \right) \times \frac{1}{4\pi w_m} \int_{\Delta\Omega_m} d\bar{\Omega} \int_{\Delta\Omega_m} d\bar{\Omega} \delta_{\mu^*,k}, \quad (20)$$

where

$$\delta_{\mu^*,k} = \begin{cases} 1 & \text{for } \mu_{k+1} \leq \mu^* - \bar{\Omega} \leq \mu_k \\ 0 & \text{otherwise,} \end{cases}$$

m and w_m denotes the Sn direction and its weight, respectively. And $\Delta\Omega_m$ is a solid angle corresponding to the direction m .

In the Monte Carlo calculation, the scattering angle and secondary energy group can be directly determined from the energy-angle distribution $I(k; g' \rightarrow g)$.



$$E_{q0} = \frac{A}{A-1} Q$$

$$E_{th} = \frac{A+1}{A} Q$$

Fig.2.1 Diagram for illustrating the scattering kinematics in the (E, E') plane and the integration limits in calculating the multi-group DDX.

3. Multi-Group DDX Library Generation Code System : PROF-DD

3.1 General Feature of PROF-DD

A calculation flow in the PROF-DD system is shown in Fig. 3.1. This system includes five steps corresponding to five independent codes. In this chapter, the descriptions are given for each step in the order of calculation flow. The outline of each step is as follows:

- MCFILEF : A control file for the PROF-DDX code, which contains energy group and angle bin structures of produced DDX, is generated by the MCFILEF code. A user should run this code initially prior to executing the job.
- RESEND : In this step, pointwise cross sections of one nuclide specified by an input data is prepared as a PROF-DDX input file. Doppler broadened resonance cross sections are calculated by the RESEND code⁶⁾ which is a modified version of RESEND.
- SPINPTF : The SPINPTF code prepares an input data file for the PROF-DDX code by combining the control file and other input data. Some parameters assigned by the MCFILEF code can be changed in this step. A weighting function is produced from the data in the control file or read from an input file.
- PROF-DDX : The PROF-DDX code is a main code in this system. This code calculates multi-group cross sections and energy-angle distributions (DDX). The calculated DDX are saved on a master PDS file with a member name assigned by the code.
- DDXLIBMK : The DDXLIBMK code reads the DDX in a master file and edits a DDX library in a specified format for a transport code such as the MORSE-DD code. This code can also print out the DDX data in the master file.

This system has functions described below.

(1) Production of multi-group DDX library

Type of processed reactions

(i) File 4 + kinematics

- elastic scattering (MT=2)
 - (n,2n) 1st scattering neutron (MT=6-9)
 - discrete level inelastic scattering (MT=51-90)
- (Two optional procedures are available. See 3.2.1.)

(ii) File 4 + File 5*

- (n,2n) direct (MT=16)
- (n,3n) (MT=17)
- (n,n'α) (MT=22)
- (n,n'3α) (MT=23)
- (n,2nα) (MT=24)
- (n,3nα) (MT=25)
- (n,n'p) (MT=28)
- (n,2n) 2nd neutron (MT=46-49)
- continuum level inelastic scattering (MT=91)

* File 6 can be processed if it is available.

(Four optional procedures are available. See 3.2.1.)

(iii) Absorption reaction

MT=102-109, 111-114

Weighting function

- (i) Maxwellian + $1/E^\alpha$ + fission spectrum
- (ii) Maxwellian + $1/E^\alpha$ + Gaussian
- (iii) Arbitrary spectrum

(2) Production of cross section library for reaction rate calculation

Type of reaction ; any reaction specified by a user

Weighting function ; the same as in (1)

In the following sections, input instructions, sample inputs and sample JCLs are given in detail for each code.

3.2 MCFILEF

The MCFILEF code prepares a control file for the PROF-DDX code. This file contains some parameters such as energy group and angle bin structures of produced DDX, which are commonly used in calculating DDX for each nuclide. Some parameters to determine a weighting function are set by the MCFILEF code.

The following processes are carried out:

- (1) Parameters which define a produced DDX library are read from cards and written on a control file.
- (2) A consistency among input data is checked.
- (3) Energy group and angle bin structures are stored in a master PDS file with member names assigned by the code. The names are fixed as follows:
 BPDSH01 : number of energy group,
 BPDSH02 : energy boundaries,
 BPDSH03 : number of angle bins,
 BPDSH04 : angle meshes.

3.2.1 Input Instruction

The following free-formatted data are read from cards.

CARD A (*)

NGRMX ; number of energy groups ($1 \leq NGRMX \leq 150$)
 MAXMU ; number of angle bins ($1 \leq MAXMU \leq 40$)
 IEOPT ; input option for energy group structure
 ≤ 0 : Energy boundaries are given from high to low
 energy in eV unit.
 ≥ 1 : Maximum energy and lethargy widths are given.
 ISW ; input option for angle meshes
 -1 : card input
 0 : equal width of $\cos \theta$,
 $\Delta\mu_k = 2/MAXMU$.
 1 : equal width of θ ,
 $\Delta\theta_k = \pi/MAXMU$.
 NO40 ; option for treatment of the NGRMX-th group (thermal
 energy group)
 -2 : NGRMX-group DDX library is produced with reac-
 tion cross sections of NGRMX-th group which are
 read from cards. Isotropic scattering is assumed
 in this group.
 -1 : NGRMX-group DDX library is produced with reac-
 tion cross sections of NGRMX-th group which are
 calculated by the PROF-DDX code. Isotropic scat-
 tering is assumed in this group.
 0 : standard treatment. (NGRMX-1)-group DDX library
 is produced with slowing down cross sections to

the NGRMX group, i.e. (NGRMX-1) reaction cross sections and (NGRMX-1)*NGRMX*MAXMU scattering probabilities are calculated.

1 : (NGRMX-1)-group DDX library is produced. The slowing down cross sections to NGRMX-th group is added to the self-group scattering of (NGRMX-1)-th group.

IUP2 ; option for calculation of energy-angle distribution based on kinematics

1 : collision density within a group is assumed to be constant in lethargy.

2 : collision density is calculated by $\sigma_x(E')\Psi_w(E')$.

IF45 ; option for calculation of energy-angle distribution from Files 4 and 5 or File 6

1 : Isotropic scattering in the laboratory system is assumed.

2 : angular distribution is taken from File 4.

3 : angular distribution is taken from File 4 and scattering probability is set as 0.0 for neutron emitted with higher energy than that determined by the two-body reaction kinematics in each direction.

4 : energy-angle distribution is obtained by integrating the energy-angle distribution data in File 6 if they are given. When they are not given, IF45 is set to be 2 by the PROFDDX code.

IPDS ; output option for a master PDS file

0 : no output on a master PDS file.

1 : numbers of energy groups and angle bins, energy group and angle bin structures are stored with member name assigned by the MCFILEF code.

CARD B (*) Enter if IEOPT \leq 0

EN(i), i=1, NGRMX+1 ; energy boundaries from high to low (eV)

CARD C (*) Enter if IEOPT \geq 1

EMAX ; upper energy boundary of 1st group (eV)

Du(i), i=1, MGRMX ; lethargy width of group i

It is required that Du(k)=n*Du(1), where n is an integer except for k=MGRMX.

CARD D (*) Enter if ISW=-1

TABMU(i), i=1, MAXMU+1 ; angle meshes from +1 to -1
 CARD E (*)
 $E_1, E_2, T, \alpha, A_1, A_2$;
 parameters to define a weighting function. The SPINPTF code generates a weighting function $\Psi_w(E)$ as follows:
 $\Psi_w(E) = C_1 E \exp(-E/kT)$ $(E \leq E_1)$
 $\Psi_w(E) = 1/E^\alpha$ $(E_1 \leq E \leq E_2)$
 $\Psi_w(E) = C_2 \exp(-E/A_1) \sinh \sqrt{A_2 E}$ $(E \geq E_2 \text{ and } A_2 > 0)$
 $\Psi_w(E) = C_2 \exp[-\{(E-A_1)/(0.426609A_2)\}^2/2]$ $(E \geq E_2 \text{ and } A_2 < 0)$

where C_1 and C_2 are determined from the continuous condition. If $E_1=0.0$, then the following values are adopted:

$$E_1=10^{-5}, E_2=2 \times 10^{-7}, T=300,$$

$$\alpha=1.0, A_1=10^{-6}, A_2=2 \times 10^{-6}.$$

If an arbitrary spectrum is used as a weighting function, this is read in by the SPINPTF code instead of using Ψ_w shown above.

CARD F (*)
 EPSPR ; error criterion. If $R_{sg} < EPSPR$, R_{sg} is set as 0.0. If $I(k; g \rightarrow g) < EPSPB (= EPSPR^2)$, I is set as 0.0. After checking, these values are recalculated.

3.2.2 Sample Input, JCL and I/O Files

The I/O files used in the MCFILEF code are shown in Fig. 3.2. Sample input and JCL to produce the DDXLIB3 library presented in Appendix are shown in Fig. 3.3.

3.3 RESEND

The RESEND code selects one nuclide from the ENDF/B formatted data file and performs resonance cross section calculations and Doppler broadening to produce temperature dependent pointwise cross section data file. This code has been developed by Nakagawa⁶⁾ of Nuclear Data Center of JAERI.

The details of this code is given in Reference (6). Some parameters which should be specified to run the PROF-DD system are described briefly in the following. The RESENDD code can be replaced by computer codes which have similar functions, for example, the LINEAR, RECENT and SIGMA1 codes⁷⁾.

3.3.1 Input Instruction for the PROF-DD System

The parameters which should be specified are as follows.

1 Job-condition cards

Job-condition inputs should be input in a form of
 ' Parameter name = value '. The parameters which should be specified are as follows:

```
MAT      ; MAT number to be selected
TEMP     ; temperature in Kelvin
ERR      ; accuracy of calculation
LSIG (=1E-10) ; option on negative cross sections
OUTF (=2) ; data set reference number of an output file
FORM     ; format of an input file
        4 : ENDF/B-IV Format
        5 : ENDF/B-V Format
OFORM (=4) ; format of an output file
OPT     (=2) ; output option
```

Values in parentheses are standard values for this system. It should be noted that the present version of PROF-DDX can process the data for a number of energy points less than 10000. A user has to set ERR by which RESENDD produces energy points less than 10000. If more points than 10000 are generated, the job is terminated by printing error messages at the following step (SPINPTF).

- 2 LABEL statement
- 3 Title (66A1)
- 4 GO statement
- 5 EOF statement
- 6 STOP statement

3.3.2 Sample Input, JCL and I/O Files

The following is a sample input for the RESENDD code used

in the system.

```
//SYSIN DD *
MAT=1272,TEMP=300.0,ERR=0.01,LSIG=1.E-10,OPT=2,FORM=4,
OFORM=4,OUTF=2
LABEL
 7-LI ENDF/B-IV
GO
EOF
STOP
/*
```

Figure 3.4 shows JCL for a continuous run of the RESENDD, SPINPTF and PROF-DDX codes. The I/O files used in the RESENDD code are shown in Fig. 3.5.

3.4 SPINPTF

The SPINPTF code produces an input data file for the PROF-DDX code from the control file generated by the MCFILEF code. The following processes are carried out:

- (1) The SPINPTF code sets up input parameters for the PROF-DDX code based on the control file and other data read from cards.
- (2) A weighting function is calculated or read from a file.
- (3) An input file for the PROF-DDX code is prepared.

3.4.1 Input Instruction

One card is read by the SPINPTF code in the free-format.

CARD A (*)

```
IPRINT ; output option
      0 : brief print.
      1 : detailed print (a lot of outputs).
IFLWX ; option on a weighting function
      0 : a weighting function is calculated with parameters
          in the control file as described in Section 3.1.
      N : a weighting function is read from a file (unit N).
IUP2 ; option for calculation of DDX based on kinematics
      See input instruction for the MCFILEF code. If
      IUP2=0, the data in a control file is adopted.
IF45 ; option for calculation of DDX from Files 4 and 5
```

See input instruction for the MCFILEF code. If IF45=0, the data in a control file is adopted.

EPSPR ; error criterion

See input instruction for the MCFILEF code. If EPSPR=0.0, the data in a control file is adopted.

If EPSPR<0.0, an error checke is not performed (i.e. EPSPR=0.0).

3.4.2 Sample input, JCL and I/O Files

Sample input and JCL are shown in Fig. 3.4. The I/O files used in the SPINPTF code is shown in Fig. 3.6. A weighting function in unit IFLXW should be given in the following form (if IFLXW ≠0.)

DATA 1 (2I6)

N1, N2 ; numbers of interpolation ranges and energy points
given for a arbitrary weighting function

DATA 2 (12I6)

(NBT(i),JNT(i),i=1,N1)

NBT(i); point number of the end point in the i-th interpolation range. NBT(N1) must be N2.

JNT(i); interpolation scheme for the i-th interpolation range. Parameter values of 1~5 have the same meaning as used in ENDF/B files.

DATA 3 (6E12.5)

(E(i),F(i),i=1,N2)

E(i) ; energy in eV of the i-th point.

The relation E(i)<E(i+1) should be satisfied.

F(i) ; weight of the i-th point.

3.5 PROF-DDX

3.5.1 Outline of PROF-DDX

The PROF-DDX code is a main code in the system, which calculates

- (1) multi-group reaction cross section weighted with the input function for neutron transport calculation,
- (2) multi-group energy-angle distribution,
- (3) multi-group reaction cross section for reaction rate calculation, and
- (4) stores these cross sections into the master PDS files

labeled with member names.

The details of input instruction are described in Section 3.5.3.

The calculation flow of the PROF-DDX code is shown in Fig. 3.7. The functions of important subroutines are briefly described below.

CROS

This subroutine calculates averaged cross sections for each group and each reaction, and stores them in a PDS file (PDSOUT2) if required.

PRODCT

Production cross section $\sigma_{pr,g'}$ and the ratio $R_{xg'} = \sigma_{xg'}/\sigma_{pr,g'}$ are calculated in this subroutine. The following check is carried out. If $R_{xg'}$ is less than EPSPR, then $R_{xg'}$ and $\sigma_{xg'}$ are set to be 0.0, where EPSPR is an input value. After this check, $\sigma_{pr,g'}$ and $R_{xg'}$ are recalculated.

TRANSM, TRANS2

As for elastic scattering (MT=2), discrete level inelastic scattering (MT=51~90) and sequential ($n,2n$) reaction (MT=6~9), for which the reaction kinematics are known, energy-angle distributions are obtained by calculating Eq.(13) in the subroutine TRANSM or TRANS2. TRANSM assumes that a collision density within a group is constant in lethargy. In TRANS2, this assumption is not used. The calculation procedure in TRANS2 is as follows.

- (1) Fine energy meshes used for the integration in Eq.(13) are determined by the following method. Incident neutron energy group, g' , is divided into $IND_{g'}$ fine energy intervals of equal lethargy width $\Delta U_{fg'}$. $IND_{g'}$ is determined such as

$$IND_{g'} = \Delta U_{g'}/\Delta U_f$$

and

$$\Delta U_f = \frac{\Delta U_1}{INK} \leq \xi = \frac{\ln \{ (A-1)/(A+1) \}^2}{50}$$

with a minimum integer INK,

where ΔU_g and A are lethargy width of the g -th group and mass of target atom, respectively.

IND_g is modified as follows:

$$IND_g = 8, \text{ if } IND_g < 8.$$

$$IND_g = 32 \text{ if } E_{th} \in g\text{'th group and if } IND_g \leq 32.$$

$$\text{Then } \Delta U_{fg} = \Delta U_g / IND_g.$$

The slowing-down energy range for each incident energy E' is divided into IND energy intervals of equal lethargy width. The following value is adopted for IND .

$$IND = \begin{cases} MAXMU * IND_0 / 2 & \text{for } MT=2 \\ IND_0 * N1 * N2 & \text{for } MT \neq 2 \end{cases}$$

$$\text{where } N1 = \begin{cases} 1.5 & \text{if } INK \geq 2 \\ 3 & \text{if } INK = 1 \end{cases}$$

$$N2 = \begin{cases} 1 & \text{for } \beta > \beta_{1U} \\ 2 & \text{for } \beta_{2L} < \beta < \beta_{1U} \text{ or } \beta_{1L} < \beta < \beta_{2U} \\ 4 & \text{for } \beta_{2L} < \beta < \beta_{2U} \end{cases}$$

where β_{1X} and β_{2X} are β values of Eq.(11) at which the lethargy width of slowing-down energy range is two and four times larger than that by elastic scattering, respectively, as shown in Fig. 3.8 for $A=7$.

- (2) The values $\sigma_x \Psi_w$, cross sections multiplied by a weighting function are calculated at each fine energy mesh point.
- (3) The P_l expansion coefficients for scattering anisotropy are calculated for each energy group as follows:

$$f_{xg}^l = \int_{\Delta E_g} f_x^l(E) \sigma_x(E) \Psi_w(E) dE / \int_{\Delta E_g} \sigma_x(E) \Psi_w(E) dE.$$

If the angular distributions are given in the form of table, the coefficients $f_x^l(E)$ are calculated by using the data in the table prior to calculating f_{xg}^l shown above.

- (4) The numerical integration with respect to E and E' is carried out based on the fine energy meshes shown in Fig. 3.9. The following algorithm is applied for each incident neutron energy group g and each reaction x .

For each fine energy interval i ($i=1, IND_{g'}$),

$$i \leftarrow IND_{g'} + 1 - i,$$

$$\Delta U^{ii} = \Delta U_{g'f} * (i \leftarrow 1) + \Delta U_{g'f} / 2,$$

$$E' = E_{g'} * \exp(-\Delta U^{ii}),$$

$$\beta = \sqrt{1 + \frac{A+1}{A} \frac{Q_x}{E'}},$$

$$\alpha_{high} = \left(\frac{A\beta+1}{A+1} \right)^2,$$

$$\alpha_{low} = \left(\frac{A\beta-1}{A+1} \right)^2,$$

$$\xi_x = \ln \frac{\alpha_{high}}{\alpha_{low}},$$

$$\Delta U_x = \xi_x / IND_0,$$

For each outgoing energy mesh boundary j ($j=1, IND_0+1$),

$$U_m = \Delta U_x * (j-1) \longrightarrow E_m = E' \exp(-U_m),$$

$$U_h = U_m - \Delta U_x / 2 \longrightarrow E_h = E' \exp(-U_h) \quad (j \neq 1),$$

$$U_l = U_m + \Delta U_x / 2 \longrightarrow E_l = E' \exp(-U_l) \quad (j \neq IND_0+1),$$

$$\Delta E = E_h - E_l,$$

$$\mu_c = \left\{ \frac{(A+1)^2}{2A} \frac{E}{E'} - \frac{A}{2} \beta (E')^2 - \frac{1}{2A} \right\} \frac{1}{\beta_x(E')},$$

$$f_{g'}(\mu_c) = \sum_{l=0}^L \frac{(2l+1)}{2} f_g^l P_l(\mu_c),$$

$$\mu = \frac{A+1}{A} \sqrt{E/E'} - \frac{A-1}{2} \sqrt{E'/E} - \frac{AQ_x}{2\sqrt{EE'}},$$

$$P_x(k; g' \rightarrow g) = P_x(k; g' \rightarrow g) + \frac{2\sigma_x(E') \Psi_w(E') f_{g'}(\mu_c) \Delta E}{(1-\alpha)\beta E'},$$

for $E_{g+1} < E_m < E_g$ and $\mu_{k+1} < \mu < \mu_k$.

After the calculation is performed for all i and j , the normalization is performed as

$$\sum_{g,k} P_x(k; g' \rightarrow g) = R_{xg'}$$

IMAT, IMATLI

These subroutines calculate Eq.(15) for reactions such as continuum inelastic scattering, for which reaction kinematics are not known. Hence, energy-angle distributions are obtained by calculating energy distribution and angle distribution separately from the data in Files 4 and 5. In IMAT calculations, however, scattering is assumed to be isotropic in the laboratory system(IF45=1). IMATLI can process both files (IF45=2 or 3). A user should specify the parameter IF45. As an optional calculation (IF45=3), IMATLI can calculate the energy-angle distribution by setting $P_x(k, g' \rightarrow g) = 0$ for $g < g_{\max}^k$, where g_{\max}^k -th group includes the energy E_{\max}^k which is the maximum energy of scattered neutron in the k -th direction predicted by the two-body reaction kinematics. File 4 is processed by the subroutine LIF4. The summation of the calculated distribution for reaction x is normalized to be $R_{xg'}$.

DDXF6

This subroutine calculates the energy-angle distribution from the data in File 6 (IF45=4). The summation of the calculated distribution for reaction x is normalized to be $R_{xg'}$.

CSWRT

The subroutine CSWRT is called after all the probabilities are calculated. This subroutine sets $I(k; g' \rightarrow g) = 0.0$ if it is less than EPSPB given by a user, and renormalize $\sum_{g,k} I(k; g' \rightarrow g)$ to be unity. Then the result is written on a file (unit 72).

PDSOUT

The subroutine PDSOUT reads the data from unit 72 and stores them on a master PDS file (PDSOUT1) with the following name:

B4aaaaACT ; MATNO, MAXMU, MAXI, MGRMX, IDMAX, ISMAX and

MAXSD(i), i=1,MAXI,
 B4aaaaAT ; ZA and AWR,
 B4aaaaTA ; production, fission, absorption, ν *fission
 and total cross sections,
 B4aaaaTB ; double-differential scattering probabilities
 $I(k, g \rightarrow g)$,

where aaaa are the NAME with 4 letters given by a user (See 3.5.2).

3.5.2 Input Instructions

The following free-formatted data are read from logical unit 80.

CARD A (*)

IOPT ; option of PROF-DDX calculation
 0 : calculation of multi-group DDX library.
 1 : calculations of multi-group DDX and responses
 libraries.
 2 : calculation of response library for reaction rate
 calculation.
 IREACT ; number of reactions to be processed (no meaning
 if IOPT=1). These are usually used as detector
 responses.

CARD B (*) Enter if IOPT ≥ 1

IMT(i), i=1,IREACT ; MT number of the i-th reaction which is
 stored in a PDS file (PDSOUT2) for the
 reaction rate calculation

CARD C (2A4) Enter if IOPT ≥ 1

TITLE(i) ; ID name assigned to the i-th reaction in a PDS
 file (PDSOUT2)
 IREACT cards are necessary.

CARD D (A4) Enter if IOPT ≤ 1

NAME ; ID name assigned to the calculated DDX in a
 master PDS file (PDSOUT1). If NAME=' ', the
 calculated DDX are not stored.

CARD E (*) Enter if NO40 = -2 (see MCFILEF)

XT,XPR,XC,XF,XNF ; total, production, absorption, fission
 and ν *fission cross sections of the
 MGRMX-th group, respectively.

3.5.3 Sample Input, JCL and I/O Files

Sample input for a simultaneous calculation of DDX and three responses is as follows:

```
//FT80F001 DD *
      1      3
      18    102    107
AAAAAAA
BBBBBBB
CCCCCCC
XXXX
/*
```

If only the DDX calculation is required, then

```
//FT80F001 DD *
      0      0
XXXX
/*
```

A sample JCL is shown in Fig. 3.4 together with those for the RESENDD and SPINPTF codes. The I/O files used in the PROF-DD code are summarized in Table 3.1.

3.6 DDXLIBMK

The DDXLIBMK code accesses the master PDS files. This code has the following functions:

- (1) to edit a DDX library from the master files for a transport code such as the MORSE-DD code,
- (2) to print out the DDX data in a master file,
- (3) to retrieve energy and angle boundaries from a control file into a master file, and
- (4) to retrieve the binary data produced by the PROF-DDX code (unit 72) into a master file.

3.6.1 Input Instruction

CARD A (*)

ISW ; function

- 1 : compilation of a DDX library for a transport code such as the MORSE-DD code.
- 2 : printout of the DDX data in a master file.
- 3 : retrieval of energy and angle boundaries from a control file into a master file.

4 : retrieval of the binary data from the PROF-DDX code
 (unit 72) into a master file.

If ISW=1, CARDs B and C are necessary.

CARD B (*)

NMAT ; number of elements to be compiled in a DDX library

NOPT ; output format

#2 : binary for MORSE-DD etc.

2 : formatted

CARD C (A4)

NAME(i) ; ID name for the i-th element in a master file,
 which is assigned by a user as an input data for
 the PROF-DDX code.

NMAT cards should be repeated.

If ISW=2, CARDs D, E and F are necessary.

CARD D (A4)

NAME ; ID name of an element to be printed out

CARD E

NINT ; number of incident groups to be printed out

CARD F (*)

IGINT(i),i=1,NINT ; incident energy group to be printed out

If ISW=3, no input card is required.

If ISW=4, CARD G is necessary.

CARD G (A4)

NAME ; ID name assigned to the present DDX data

3.6.2 Sample Input, JCL and I/O Files

Sample input and JCL for producing the DDXLIB3 library
 are shown in Fig. 3.10. The I/O files are shown in Fig. 3.11.

3.6.3 Structure of DDX Library

The DDX library is edited by the DDXLIBMK code in the following form.

```

1, NMAT
  MAXI, IDUMMY, IDUMMY, MATNO, (Title(i), i=1, 12)
  (MAXSD(i), i=1, MAXI)
  ( $\sigma_{prg}$ ,  $\sigma_{fg}$ ,  $\sigma_{ag}$ ,  $\nu\sigma_{fg}$ ,  $\sigma_{tg}$ , i=1, MAXI)

1, MAXI
  (( $I(k;g \rightarrow g)$ , k=1, MAXMU), g=1, MAXSD(g))

```

When this library is used in transport calculation, cross section data for each element are identified by MATNO which is a Material Number (MAT) given for each element in the evaluated nuclear data library.

When NOPT on CARD B is equal to 2, the library with the following format is generated.

```

1, NMAT
  MAXI, IDUMMY, IDUMMY, MATNO, (Title(i), i=1, 12) (4I6, 12A4)
  (MAXSD(i), i=1, MAXI) (12I6)
  ( $\sigma_{prg}$ ,  $\sigma_{fg}$ ,  $\sigma_{ag}$ ,  $\nu\sigma_{fg}$ ,  $\sigma_{tg}$ , i=1, MAXI) (10E12.5)

1, MAXI
  (( $I(k;g \rightarrow g)$ , k=1, MAXMU), g=1, MAXSD(g)) (10E12.5)

```

Table 3.1 PROF-DDX file requirements

Logical unit	Contents	Remarks	I/O
PDSOUT1	DDX data	Master PDS file	0
PDSOUT2	Response	PDS file	0
5	Card-image input	Output of SPINPTF < FT08F001 >	I
6	LP output		0
8	ENDF/B file (pointwise data)	Output of RESEND < OUTF >	I
72	Scratch	Temporary output of DDX	I/O
80	Card-image input	Option for fileout etc.	I
90	Scratch	Check write (DUMMY)	0
1 - 4		Temporary storage for	
51 53 54	Scratch	nuclear data	I/O
55 74 75		(MF = 3, 4 and 5)	

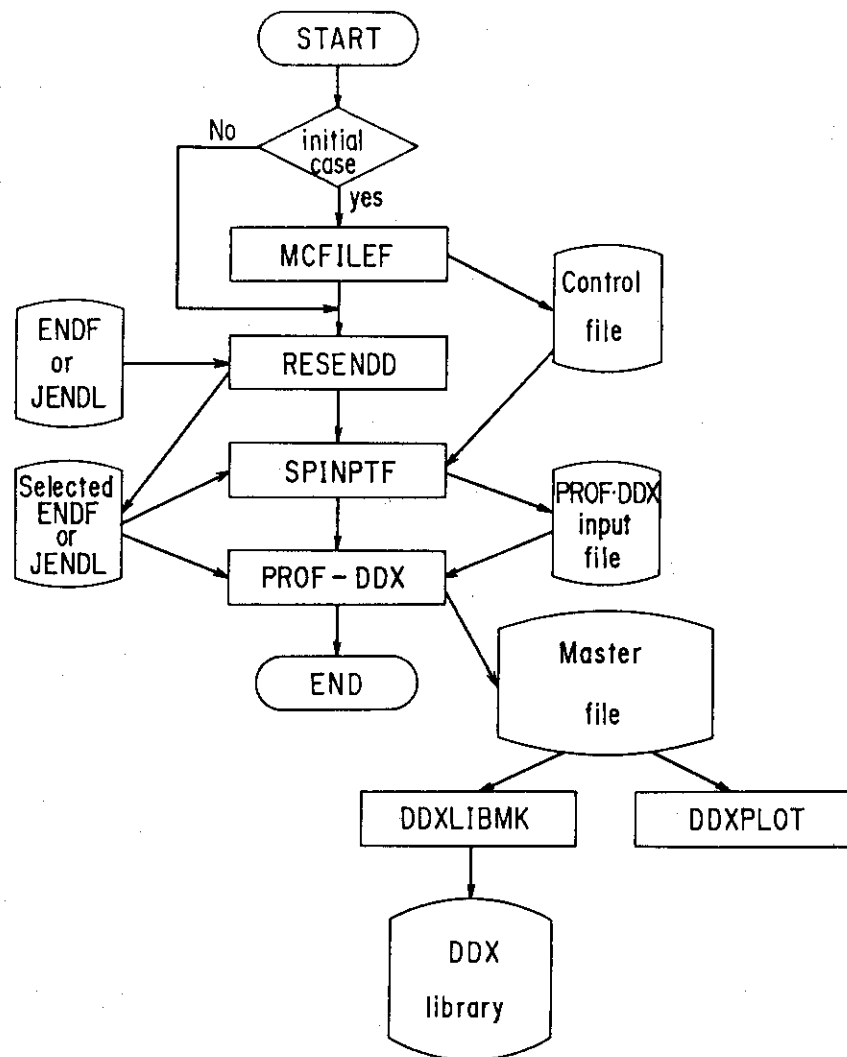


Fig.3.1 Flow of the PROF-DD system.

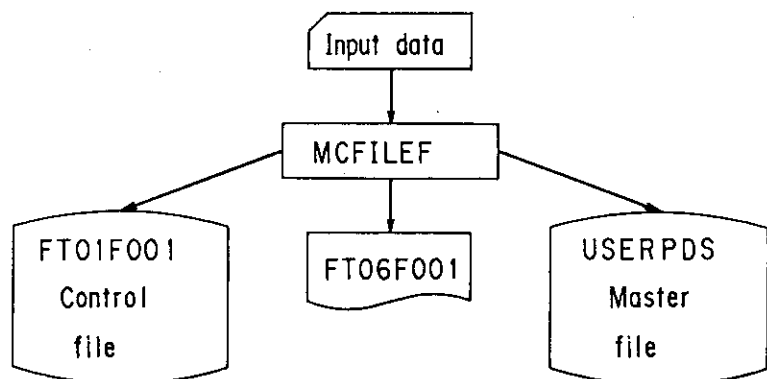


Fig.3.2 I/O files for the MCFILEF code.

```

//JCLG JOB
// EXEC JCLG
//SYSIN DD DATA,DLM='++'
// JUSER XXXXXXXX,TA.MORI,0431.110
T.1 C.O W.O I.3
OPTP MSGCLASS=R,PASSWORD=XX
//*****'J3803.DDX.CNTL(MCFILEF)' ****
//*
//*      ****M C F I L E F ****
//*      ****
//*
//MCFILEF EXEC LMGO,LM='J3803.PROFDD',PNM=MCFILEF
//----- USERPDS : MASTER FILE -----
//USERPDS DD DSN=J3803.DDXLIB3.PDS125G.DATA,DISP=MOD
//*
//----- FT01F001 : CONTROL FILE -----
//FT01F001 DD DSN=J3803.DDXLIB3.CNTL.DATA,DISP=OLD
//*
//SYSIN DD *
 125 20 1 0 -1 2 2 1 / #A
 1.6487E+07 32(0.015625) 28(0.0625) 36(0.125) 12(0.25) 16(0.5) 10.38/#C
 3.2241E-1 2.E+7 300. 1. 1.E+06 2.E-6 / #E WEIGHTING FUNCTION
 1.E-10 / #F
++
//
```

Fig.3.3 Sample JCL and input data for the MCFILEF code.

```

//JCLG JOB
// EXEC JCLG
//SYSIN DD DATA,DLM='++'
// JUSER [REDACTED],T.MORI,0431.110
    T.5 C.4 W.2 P.0 I.4
    OPTP MSGCLASS=R,PASSWORD=
//***** 'J3803.DDX.CNTL(PROFUP)' ****
//PROC=J2608.PROCLIB.CNTL
/*
//* ****
//* *** R E S E N D D ***
//* *** ****
//* ****
//* ****
/*
//RESENDD EXEC RESEND
//----- FT01F001 : ENDF/B -----
//FT01F001 DD DSN=J3770.J3PR1.DATA(LI6),LABEL=(,,,IN),DISP=SHR
//*T01F001 DD DSN=J1615.ENDFB408.DATA,LABEL=(,,,IN),DISP=SHR
/*
//----- FT02F001 : SELECTED ENDF/B POINTWISE DATA -----
//FT02F001 DD DSN=&&BT0B,SPACE=(TRK,(100,10)),DISP=(NEW,PASS),
//   DCB=(RECFM=FB,LRECL=80,BLKSIZE=3200,BUFL=3200,DSORG=PS),UNIT=WK10
/*
//SYSIN DD *
  MAT= 306,TEMP=300.0,ERR=0.01,LSIG=1.E-10,OUTF=2,OPT=2,FORM=4,OFORM=4
LABEL
LI-6J3
GO
EOF
STOP
/*
//*
//* ****
//* *** S P I N P T F ***
//* *** ****
//* ****
/*
//SPINPTM EXEC LMGO,LM='J3803.PROFDD',PNM=SPINPTF
//----- FT01F001 : CONTROL FILE FROM MCFILEF -----
//FT01F001 DD DSN=J3803.DDXLIB3.CNTL.DATA,DISP=SHR,LABEL=(,,,IN)
/*
//----- FT02F001 : SELECTED ENDF/B POINTWISE DATA FROM RESENDD --
//FT02F001 DD DSN=&&BT0B,DISP=(OLD,PASS)
/*
//----- FT08F001 : INPUT DATA FILE FOR PROFDDX -----
//FT08F001 DD DSN=&&DATA,SPACE=(TRK,(100,10)),DISP=(NEW,PASS),
//   DCB=(RECFM=FB,LRECL=80,BLKSIZE=3200,BUFL=3200,DSORG=PS),UNIT=WK10
/*
//SYSIN DD *
  0 0 0 4 0.0          / IPRNT IFLXW IUP2 IF45 EPSPR
/*
/*

```

Fig.3.4 JCLs and input data for the RESEND, SPINPTF, and PROF-DDX codes.

```

//* ****
//* ****
//* **** P R O F - D D X ****
//* ****
//* ****
//*
// EXEC ANY
//PROFDDX EXEC LMGO,LM='J3803.PROFDD',PNM=PROFDDX,OBSIZE=137
//----- FT05F001 : INPUT DATA FILE FROM SPINPTF -----
//FT05F001 DD DSN=&&DATA,DISP=(OLD,DELETE)
//*
//----- PDSOUT1 : MASTER PDS FILE ( DDX ) -----
// PDSOUT2 : PDS FILE ( REACTION CX DATA )
//PDSOUT1 DD DSN=J3803.DDXLIB3.PDS125G.DATA,DISP=SHR
//PDSOUT2 DD DSN=J3803.PDSTEMP.DATA,DISP=SHR
//*
//----- FT01 --> FT75 : WORK FILE -----
//FT01F001 DD DSN=&&WK01,UNIT=WK10,SPACE=(TRK,(200,50))
//FT02F001 DD DSN=&&WK02,UNIT=WK10,SPACE=(TRK,(200,50))
//FT03F001 DD DSN=&&WK03,UNIT=WK10,SPACE=(TRK,(200,50))
//FT04F001 DD DSN=&&WK04,UNIT=WK10,SPACE=(TRK,(200,50))
//FT08F001 DD DSN=&&BT0B,DISP=(OLD,DELETE)
//FT51F001 DD DSN=&&WK51,UNIT=WK10,SPACE=(TRK,(200,50))
//FT53F001 DD DSN=&&WK53,UNIT=WK10,SPACE=(TRK,(200,50))
//FT54F001 DD DSN=&&WK54,UNIT=WK10,SPACE=(TRK,(200,50))
//FT55F001 DD DSN=&&WK55,UNIT=WK10,SPACE=(TRK,(200,50))
//FT74F001 DD DSN=&&WK74,UNIT=WK10,SPACE=(TRK,(200,50))
//FT75F001 DD DSN=&&WK75,UNIT=WK10,SPACE=(TRK,(200,50))
//*
//----- FT72F001 : TEMPORARY OUTPUT OF DDX DATA -----
//FT72F001 DD DSN=&&WK72,UNIT=WK10,SPACE=(TRK,(50,10))
//*
//----- FT90F001 : CHECK WRITE ( FB FILE ) -----
//FT90F001 DD DUMMY
//*T90F001 DD SYSOUT=*
//*
//----- FT80F001 : CARD-IMAGE INPUT FILE -----
//FT80F001 DD *
      0      0
LI6D
++
//
```

Fig. 3.4 (continued)

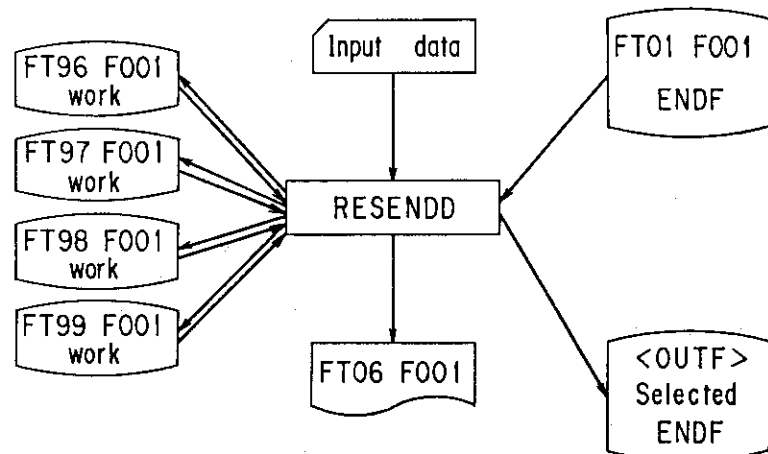


Fig.3.5 I/O files for the RESEND code.

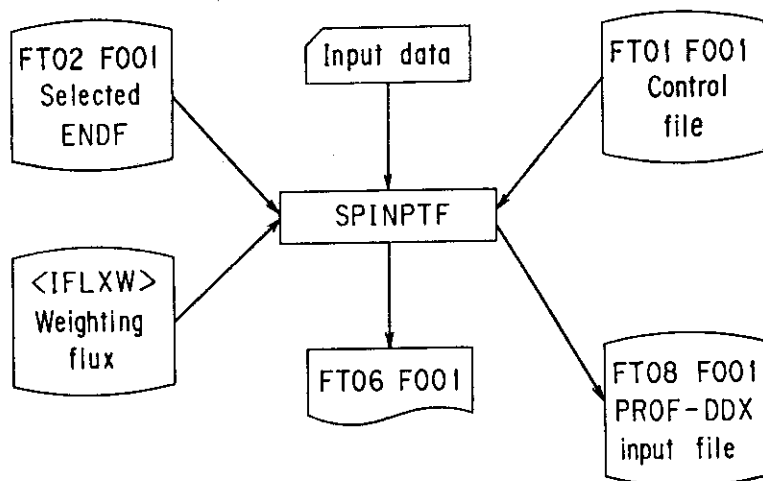


Fig.3.6 I/O files for the SPINPTF code.

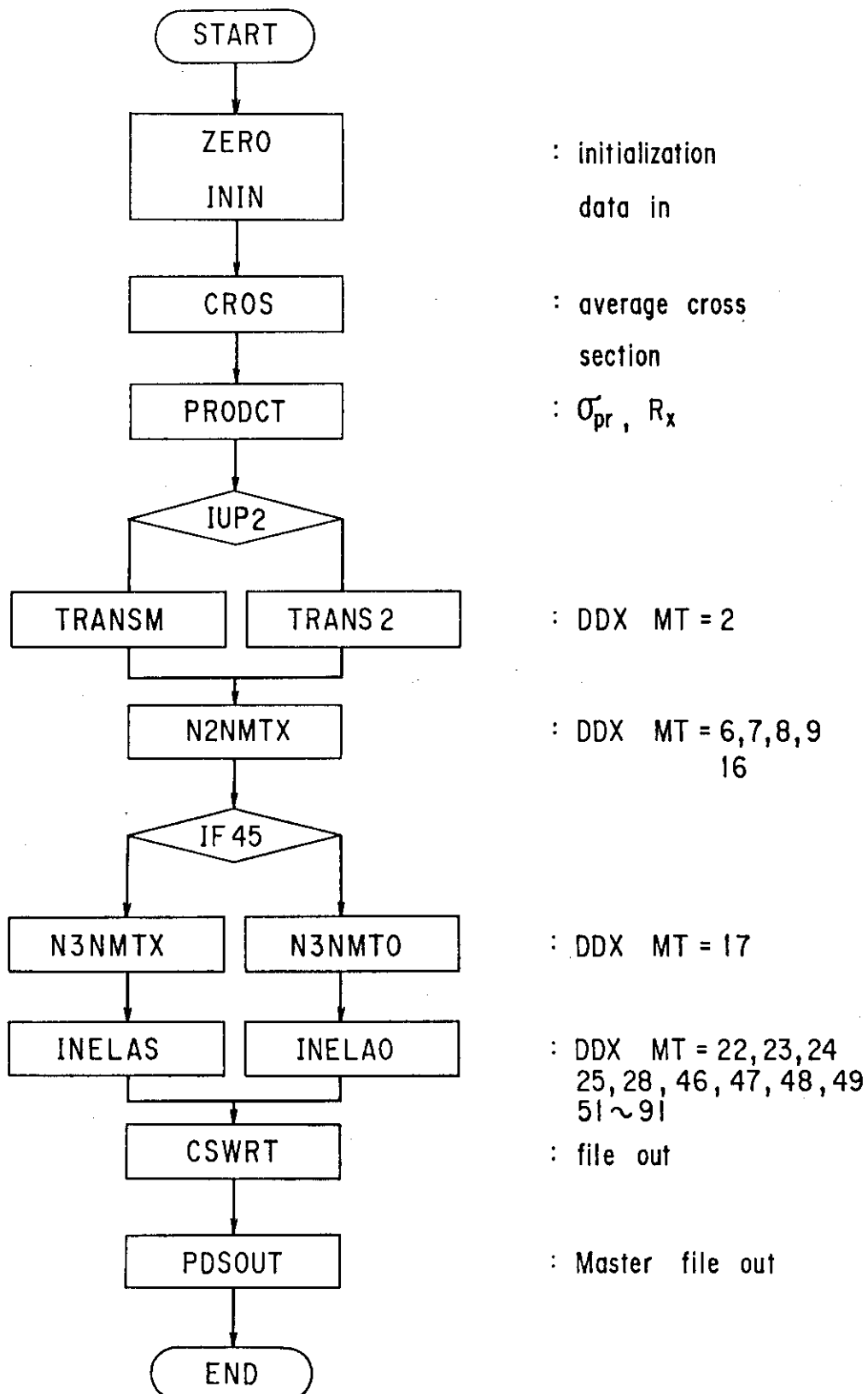
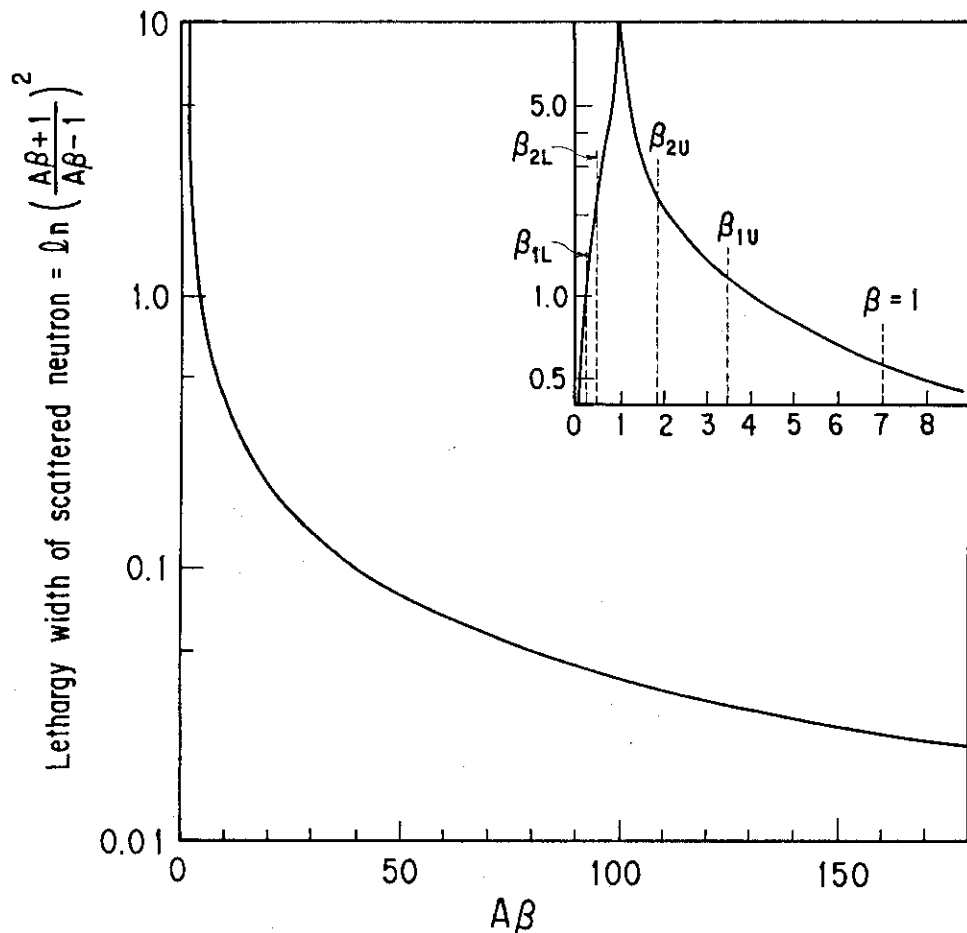
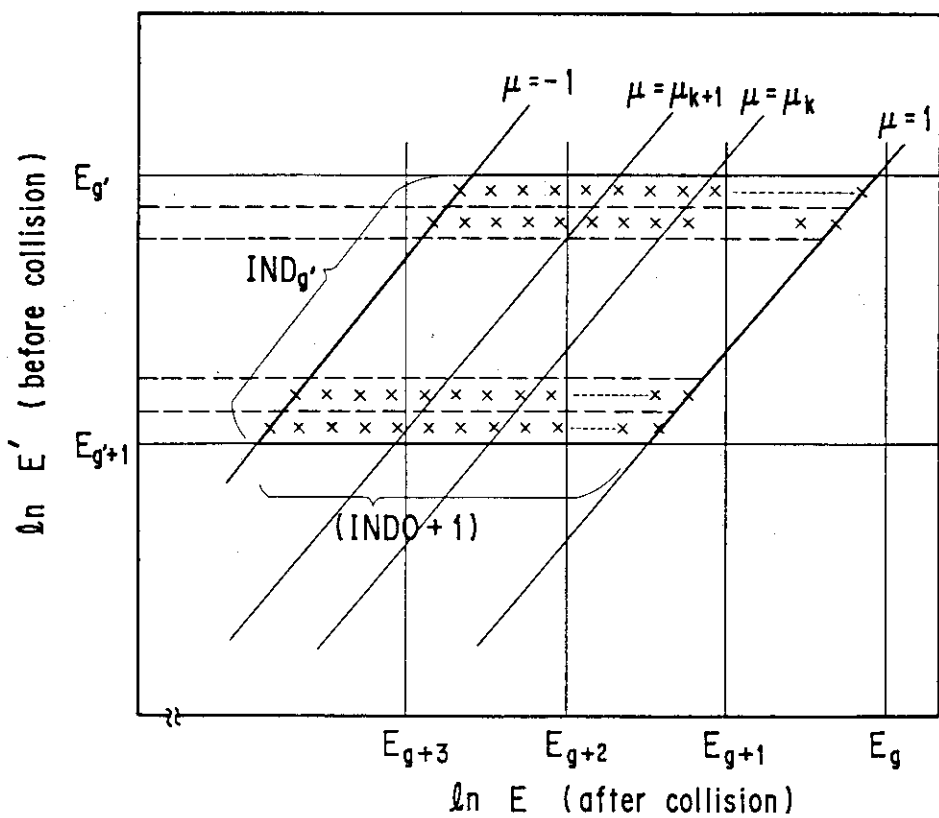


Fig.3.7 Calculation flow in the PROF-DDX code.

Fig. 3.8 Lethargy width of scattered neutrons versus $A\beta$.Fig. 3.9 Fine energy meshes for numerical integration with respect to E and E' in the subroutines TRANSM and TRANS2.

```

//JCLG JOB
// EXEC JCLG
//SYSIN DD DATA,DLM='++'
// JUSER XXXXXXXX,TA.MORI,0431.110
    T.2 C.3 W.O P.O I.7 NGT
    OOPTP MSGCLASS=R,PASSWORD=XX
//***** J3803.DDX.CNTL(DDXLIBMK) *****
//* PRODUCTION OF DDX LIBRARY
//*
//* ****
//*      * D D X L I B M K *
//* ****
//*
//DDXLIBMK EXEC LMGO,LM=J3803.PROFDD,PNM=DDXLIBMK
//*
//----- FT08F001 : DDX LIBRARY -----
//FT08F001 DD DSN=J3803.DDXLIB3.DATA,DISP=OLD,
// DCB=(RECFM=VBS,LRECL=X,BLKSIZE=23476)
//*
//----- USERPDS : MASTER FILE -----
//USERPDS DD DSN=J3803.DDXLIB3.PDS125G.DATA,DISP=SHR,LABEL=(,,,IN)
//*
//SYSIN DD *
    1
  29 1
1269
1271
1272
1274
1289
1275
1276
1156
1280
1193
1194
1150
1195
1191
1192
1190
1197
1295
1287
1288
0306
0307
0409
0612
0816
2400
2600
2800
1277
/*
++
//
```

Fig.3.10 Sample JCL and input data for the DDXLIBMK code
(Compilation of a DDX library).

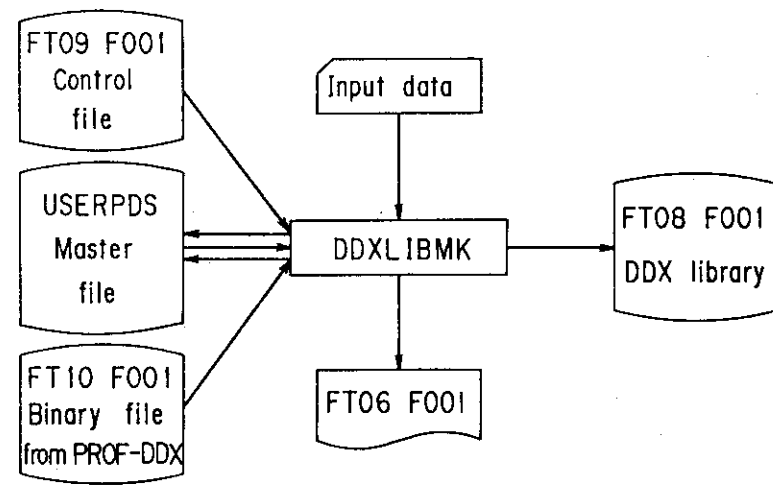


Fig.3.11 I/O files for the DDXLIBMK code.

4. Auxiliary Programs

4.1. DDXPLOT

The DDXPLOT code can draw the following types of figures for the data in master PDS files.

- (1) three dimensional feature of DDX data for a specified incident energy in a master file (from logical unit USERPDS).
- (2) energy distribution in a specified direction.
- (3) outgoing-energy distribution integrated over scattering angle.
- (4) angular distribution in a specified outgoing energy group.
- (5) angular distribution integrated over outgoing energy.
- (6) experimental values of DDX.

In the cases of (2) ~ (6), the DDXPLOT code produces an input data file for the plotting program PLTJOINT. The I/O files used and data flow are shown in Fig. 4.1.

The input for the DDXPLOT code is as follows:

CARD A (A4,I4)

NAME ; ID name for DDX data. If NAME='END', job is terminated. This is used for drawing the three dimensional feature of DDX.

IDWNMX ;

< 0 : 2-dimensional figure.

≥ 0 : 3-dimensional feature.

As a slowing-down group, IDWNMX is assumed. If IDWNMX=0, IDWNMX is set as 20.

CARD B (20A4)

TIT ; title of the figure.

If IDWNMX ≥ 0 (3-D feature), the following card is necessary.

CARD C (*)

NG ; incident neutron energy group.

If NG ≤ 0 , job is terminated.

ILOG ; option for z-axis.

0 : linear

1 : log

IZERO ; slowing-down probabilities for the first IZERO groups are set as 0.0.

This card is repeated until $NG \leq 0$. A negative NG is found, CARD A is read again.

If $IDWNMX < 0$ (2-D figure), the following cards (D to P4) are necessary.

CARD D (A4)

NAME ; ID name for calculated DDX data in a PDS file. If NAME='EXP', experimental DDX data are read from cards or file. When all DDX data for this figure are already input, NAME should be 'END'. Then input of some parameters for plotting the data follows (See CARD P1).

When NAME=ID name in a PDS file.

CARD E (2A4)

FNAME ; reference name for a master PDS file.

CARD F (*)

NGG ; incident neutron energy group.

IPOPT ;

>0 : energy distribution (/ lethargy).

<0 : energy distribution (/ eV).

=0 : angular distribution (/Str.).

IINT ;

>0 : angular distribution of (NNG->NNG+IINT-1) if IPOPT=0.

energy distribution of IINT-th direction if IPOPT<0.

=0 : integrated distribution with respect to energy or angle.

CARD G (5A4)

SUBTIT ; subtitle of the present data

A pair of CARDs F and G are repeated until $NGG \leq 0$. If a negative NGG on CARD F is found, CARD D is read again.

When NAME='EXP'.

CARD H (*)

IPOPT ; input option for experimental data

0 : from a file.

N : from cards. N data are read.

CARD H1 (5A4)

SUBTIT ; subtitle of the present data

CARD H2 (*) Enter if IPOPT=0

I ; data number.

XX ; x value.

YY ; y value.

ERR ; fractional error in YY.

IPOPT cards should be repeated.

Following CARD H2, CARD D is read again.

CARD H3 (2A4,2I3) Enter if IPOPT=0

IENT ; entry number of the data.

ISUB ; sub-entry number of the data.

NEXP ; number of experimental data.

NTYP ; output option

0/1 = unit lethargy/ unit energy.

Following CARD H3, CARD D is read again.

A set of CARDS P1 to P4 is read for each 2-dimensional figure.

CARD P1 (*)

XMI ; minimum value of x

If 0.0 is given, XMI is automatically set.

XMA ; maximum value of x

If 0.0 is given, XMA is automatically set.

YMI ; minimum value of y

If 0.0 is given, YMI is automatically set.

YMA ; maximum value of y

If 0.0 is given, YMA is automatically set.

STLT ; X-position of subtitle(left)

If 0.0 is given, subtitle is positioned at the center of X-axis.

STBM ; Y-position of subtitle(bottom)

If 0.0 is given, subtitle is positioned above the figure.

CARD P2 (*)

KP1 ; option for main lines

2 : thick line

1 : thin line

KP2 ; option for grid lines

2 : thick line

```

    1 : thin line
KP3      ; in future use
SX       ; length of X-axis (cm)
SY       ; length of Y-axis (cm)
SXO     ; X-length of frame (cm)
SYO     ; Y-length of frame (cm)
SIM     ; height of letter for main title (cm)
SIX     ; height of letter for X-title (cm)
SIY     ; height of letter for Y-title (cm)
SIS     ; height of letter for subtitle (cm)
SLI     ; height of letter for axes in linear scale (cm)
SLO     ; height of letter for axes in log scale (cm)

CARD P3 (20A4)
XTIT    ; title for X-axis
CARD P4 (20A4)
YTIT    ; title for Y-axis
Following CARD P4, CARD A is read again.

```

Sample input and JCL are shown in Fig.4.2. Output figures are shown in Figs.4.3.

4.2 Dump of DDX Data in Master File

The DDXLIBMK code can be used for this purpose. The input instructions are given in Section 3.6.2. Sample input and output are shown in Figs. 4.4 and 4.5.

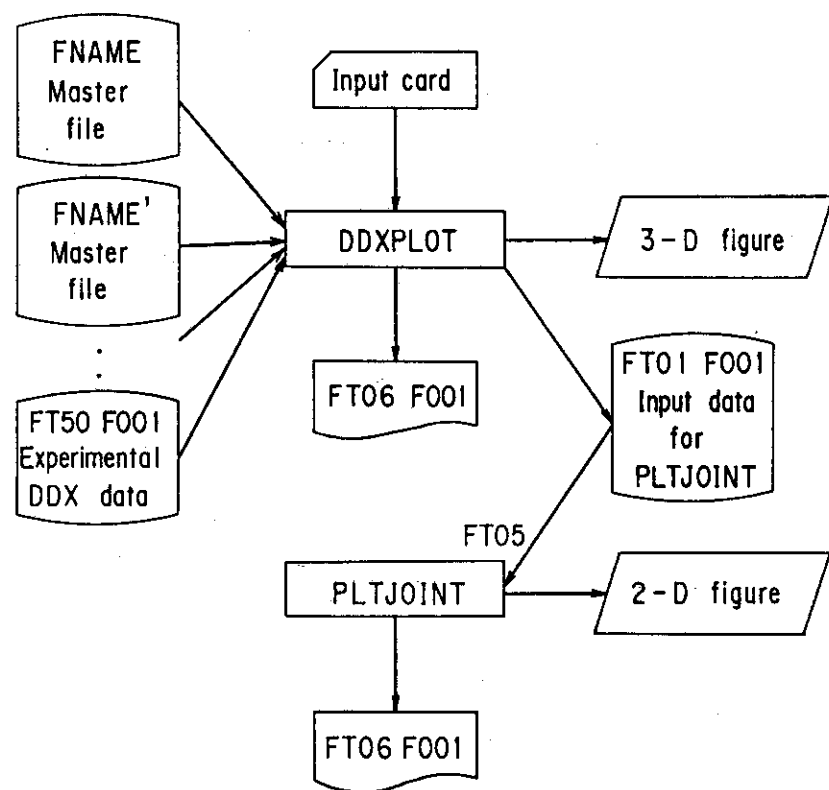


Fig.4.1 Flow of plotting by the DDXPLOT and PLTJOINT codes.

```

//JCLG JOB
// EXEC JCLG
//SYSIN DD DATA,DLM='++'
// JUSER xxxxxxxx,T.MORI,0431.110,FBREACT
  I.5 C.3 T.2 W.O GRP NLP
  OOPT MSGCLASS=R,PASSWORD=xx
//*****'J3803-DDX2.CNTL(DDXPLOT)' *****
//*
//*      ***** D D X P L O T      *
//*      ***** *****
//*
//DDXPLOT EXEC LMGO,LM='J3803.PROFDD',PNM=DDXPLOT
//----- USERPDS : MASTER FILE 1 -----
//USERPDS DD DSN=J3803.PROFDDX.PDS124G.DATA,DISP=SHR,LABEL=(,,,IN)
//          DD DSN=J3803.DDXLIB3.PDS125G.DATA,DISP=SHR,LABEL=(,,,IN)
//----- DDXLIB1 : MASTER FILE 2 -----
//DDXLIB1 DD DSN=J3803.PROFDDXJ.PDS124G.DATA,DISP=SHR,LABEL=(,,,IN)
//----- DDXLIB3 : MASTER FILE 3 -----
//DDXLIB3 DD DSN=J3803.DDXLIB3.PDS125G.DATA,DISP=SHR,LABEL=(,,,IN)
//----- DDXLIB4 : MASTER FILE 4 -----
//DDXLIB4 DD DSN=J3803.PDSTEMP.DATA,DISP=SHR,LABEL=(,,,IN)
//*
//----- FT09F001 : CHECK WRITE -----
//FT09F001 DD DUMMY
//*
//----- FT01F001 : INPUT DATA FOR PLTJOINT -----
//FT01F001 DD DSN=&&WK1,DISP=(NEW,PASS),UNIT=WK10,
//          DCB=(RECFM=FB,LRECL=80,BLKSIZE=3120),SPACE=(TRK,(10,10))
//*
// EXPAND GRNLP,SYSPUT=M
//*
//----- DATA FOR DDXPLOT -----
//*
//SYSIN DD *
FIG1 -1
Energy distribution of Lithium-7
0307
DDXLIB1
 8 3 0
DDXLIB1(J3PR1 8G)
-1 0 0
0307
DDXLIB3
 8 3 0
DDXLIB3(J3PR1 8G)
-1 0 0
LI7E
DDXLIB4
 8 3 0
DDXLIB4(J3PR1 8G)
-1 0 0
END
 2 3 1 1
1.1E6  0.9E8   1.1E-2 .0    0.0    0.0
2 1 1 20.0 15.0 28.0 20.0  0.3  0.3  0.3  0.3  0.3
Energy (eV)
P(E'->E) (barn/leth.)
FIG2 -1
Energy Distribution of Lithium-7 (DDX-Angle17)
0307
DDXLIB1
 8 3 17
DDXLIB1(J3PR1 8G)
-1 0 0
0307
DDXLIB3
 8 3 17
DDXLIB3(J3PR1 8G)
-1 0 0
LI7E
DDXLIB4
 8 3 17
DDXLIB4(J3PR1 8G)
-1 0 0
END

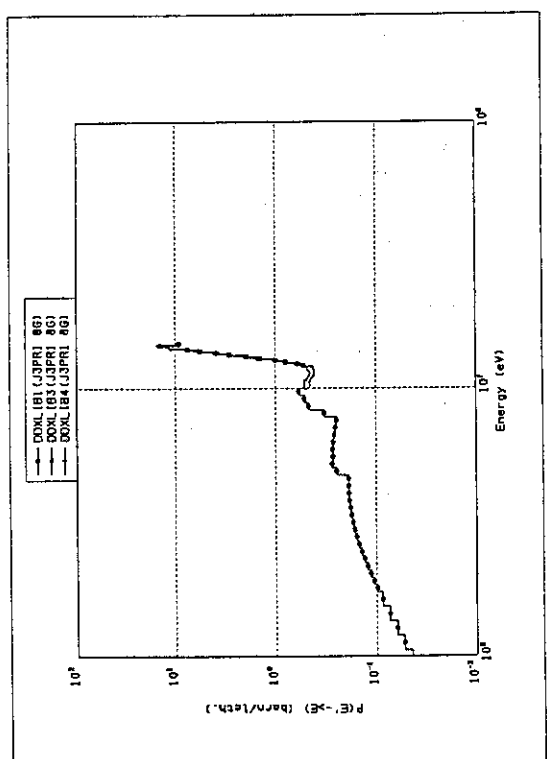
```

Fig.4.2 Sample JCLs and input data for the DDXPLOT and PLTJOINT codes.

```

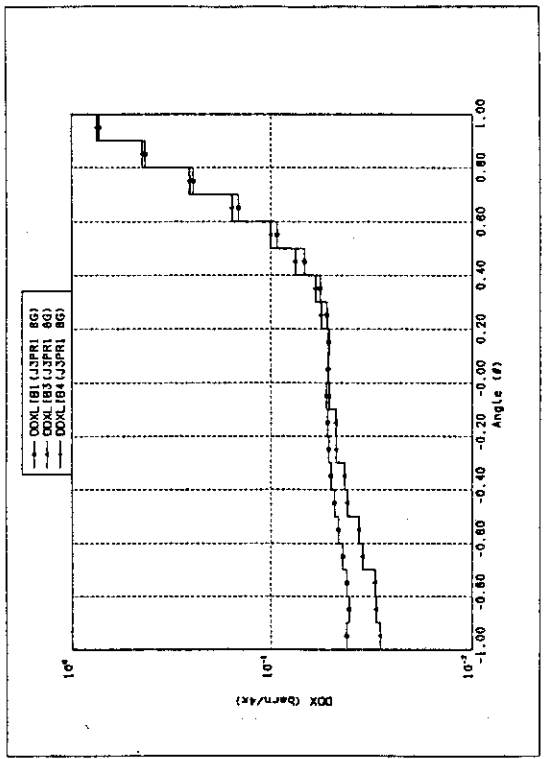
2 3 1 1
1.1E5 0.9E8 1.1E-5 0.0 0.0 0.0
2 1 1 20.0 15.0 28.0 20.0 0.3 0.3 0.3 0.3 0.3 0.3
Energy (eV)
DDX (barn/Leth./4fpf)
FIG3 -1
Angle Distribution of Lithium-7
0307
DDXLIB1
8 0 0
DDXLIB1(J3PR1 8G)
-1 0 0
0307
DDXLIB3
8 0 0
DDXLIB3(J3PR1 8G)
-1 0 0
L17E
DDXLIB4
8 0 0
DDXLIB4(J3PR1 8G)
-1 0 0
END
2 3 1 1
0.0 0.0 0.0 0.0 0.0 0.0
2 1 1 20.0 15.0 28.0 20.0 0.3 0.3 0.3 0.3 0.3 0.3
Angle (fcf)
DDX (barn/4fpf)
0307 50
DDX OF LITHIUM-7 IN DDXLIB3 (JENDL-3PR1)
8 1 0
0 0 0
END
//----- DATA END FOR DDXPLOT -----
//*
//***** P L T J O I N T : 2-D FIGURE *****
//*****
//PLTJOINT EXEC LMGO,LM=J2350.PLTJOINT,PNM=PLTJOINT
//*
//FT06F001 DD DUMMY
//----- FT11 - FT22 : WORK -----
//FT11F001 DD DISP=(NEW,PASS),SPACE=(TRK,(50,10)),UNIT=WK10
//FT12F001 DD DISP=(NEW,PASS),SPACE=(TRK,(50,10)),UNIT=WK10
//FT13F001 DD DISP=(NEW,PASS),SPACE=(TRK,(50,10)),UNIT=WK10
//FT14F001 DD DISP=(NEW,PASS),SPACE=(TRK,(50,10)),UNIT=WK10
//FT15F001 DD DISP=(NEW,PASS),SPACE=(TRK,(50,10)),UNIT=WK10
//FT16F001 DD DISP=(NEW,PASS),SPACE=(TRK,(50,10)),UNIT=WK10
//FT17F001 DD DISP=(NEW,PASS),SPACE=(TRK,(50,10)),UNIT=WK10
//FT18F001 DD DISP=(NEW,PASS),SPACE=(TRK,(50,10)),UNIT=WK10
//FT19F001 DD DISP=(NEW,PASS),SPACE=(TRK,(50,10)),UNIT=WK10
//FT20F001 DD DISP=(NEW,PASS),SPACE=(TRK,(50,10)),UNIT=WK10
//FT21F001 DD DISP=(NEW,PASS),SPACE=(TRK,(50,10)),UNIT=WK10
//FT22F001 DD DISP=(NEW,PASS),SPACE=(TRK,(50,10)),UNIT=WK10
//*
// EXPAND GRNLP,SYSPUT=M
//----- SYSIN : INPUT FILE FROM DDXPLOT -----
//SYSIN DD DSN=&&WK1,DISP=SHR
/*
++
//
```

Fig. 4.2 (continued)

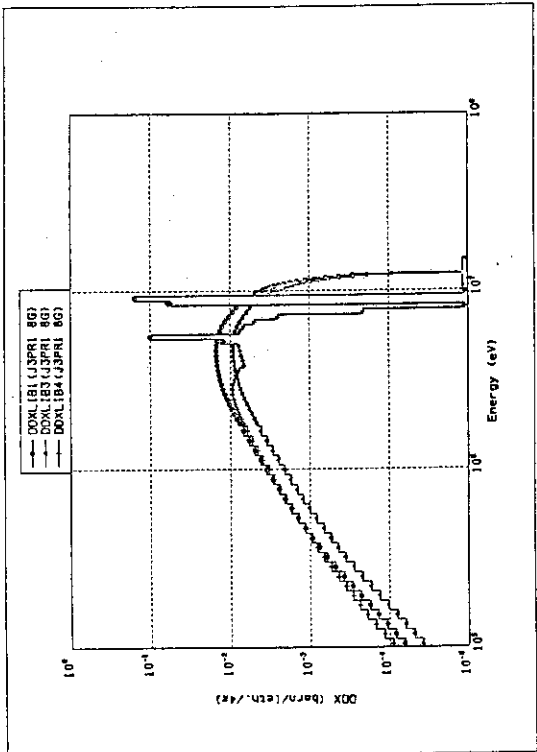


(a)

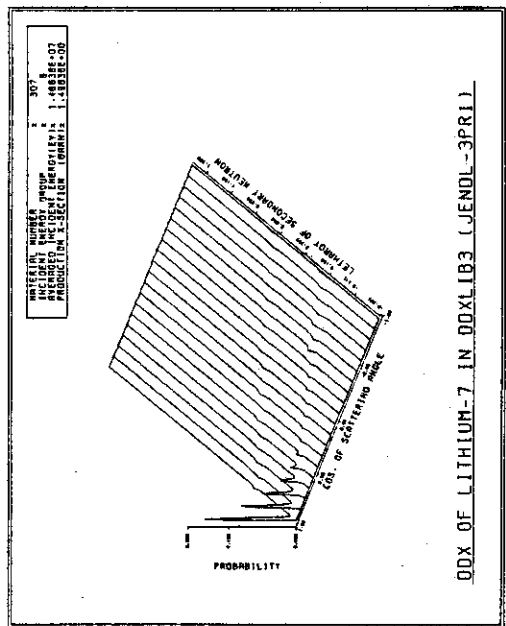
Angle Distribution of Lithium-7



(c)



(b)



(d)

Fig. 4.3 Sample output data of the DDXPLOT and PLTJOINT codes with input data in Fig. 4.2.

```
//JCLG JOB
// EXEC JCLG
//SYSIN DD DATA,DLM='++'
// JUSER XXXXXXXX,T.MORI,0431.110
  T.O C.3 W.1 I.3
  OPTP MSGCLASS=R,PASSWORD=XX
/*
/**      **** * ***** * ***** * ***** * ***** *
/**      *          D D X L I B M K          *
/**      * ***** * ***** * ***** * ***** * ***** *
/**
// EXEC LMGO,LM=J3803.PROFDD,PNM=DDXLIBMK
/*
----- USERPDS : MASTER FILE -----
//USERPDS DD DSN=J3803.DDXLIB3.PDS125G.DATA,DISP=SHR,LABEL=(,,,IN)
//          DD DSN=J3803.PDSTEMP.DATA,DISP=SHR,LABEL=(,,,IN)
/*
//SYSIN DD *
  2
0306
  11
    1     11     21     31     41     51     101    111    121    124    125
/*
+++
//
```

Fig.4.4 Sample JCL and input data for the DDXLIBMK code
(Dump of DDX in a PDS file).

MULTI-GROUP CROSS SECTION						
GROUP	PRODUCTION	FISSION	CAPTURE	NU-FISSION	TOTAL	
1	1.4083E+00	0.0	2.7944E-02	0.0	1.3362E+00	
2	1.4189E+00	0.0	2.8868E-02	0.0	1.3478E+00	
3	1.4293E+00	0.0	2.9751E-02	0.0	1.3593E+00	
4	1.4395E+00	0.0	3.0461E-02	0.0	1.3705E+00	
5	1.4498E+00	0.0	3.1130E-02	0.0	1.3817E+00	
6	1.4600E+00	0.0	3.1784E-02	0.0	1.3928E+00	
7	1.4702E+00	0.0	3.2422E-02	0.0	1.4039E+00	
8	1.4803E+00	0.0	3.3050E-02	0.0	1.4150E+00	
9	1.4906E+00	0.0	3.3669E-02	0.0	1.4261E+00	
10	1.5018E+00	0.0	3.4278E-02	0.0	1.4383E+00	
11	1.5134E+00	0.0	3.4917E-02	0.0	1.4511E+00	
12	1.5234E+00	0.0	3.5584E-02	0.0	1.4639E+00	
13	1.5330E+00	0.0	3.6208E-02	0.0	1.4764E+00	
14	1.5426E+00	0.0	3.6777E-02	0.0	1.4889E+00	
15	1.5526E+00	0.0	3.7324E-02	0.0	1.5017E+00	
16	1.5625E+00	0.0	3.7864E-02	0.0	1.5148E+00	
17	1.5709E+00	0.0	3.8416E-02	0.0	1.5274E+00	
18	1.5793E+00	0.0	3.9004E-02	0.0	1.5398E+00	
19	1.5877E+00	0.0	3.9583E-02	0.0	1.5524E+00	
20	1.5959E+00	0.0	4.0156E-02	0.0	1.5645E+00	
21	1.6039E+00	0.0	4.0719E-02	0.0	1.5764E+00	
22	1.6119E+00	0.0	4.1273E-02	0.0	1.5880E+00	
23	1.6199E+00	0.0	4.1817E-02	0.0	1.5995E+00	
24	1.6279E+00	0.0	4.2364E-02	0.0	1.6109E+00	
25	1.6357E+00	0.0	4.2941E-02	0.0	1.6222E+00	
26	1.6435E+00	0.0	4.3539E-02	0.0	1.6335E+00	
27	1.6515E+00	0.0	4.4138E-02	0.0	1.6447E+00	
28	1.6593E+00	0.0	4.4768E-02	0.0	1.6558E+00	
29	1.6671E+00	0.0	4.5394E-02	0.0	1.6667E+00	
30	1.6749E+00	0.0	4.6012E-02	0.0	1.6776E+00	
31	1.6831E+00	0.0	4.6621E-02	0.0	1.6888E+00	
32	1.6917E+00	0.0	4.7219E-02	0.0	1.7005E+00	
33	1.7125E+00	0.0	4.8674E-02	0.0	1.7279E+00	
34	1.7462E+00	0.0	5.1105E-02	0.0	1.7717E+00	
35	1.7772E+00	0.0	5.4678E-02	0.0	1.8126E+00	
36	1.8055E+00	0.0	5.9284E-02	0.0	1.8511E+00	
37	1.8334E+00	0.0	6.4536E-02	0.0	1.8890E+00	
38	1.8625E+00	0.0	7.0338E-02	0.0	1.9283E+00	
39	1.8921E+00	0.0	7.6334E-02	0.0	1.9677E+00	
40	1.9231E+00	0.0	8.2557E-02	0.0	2.0057E+00	
41	1.9507E+00	0.0	8.8802E-02	0.0	2.0393E+00	
42	1.9704E+00	0.0	9.6780E-02	0.0	2.0672E+00	
43	1.9799E+00	0.0	1.0753E-01	0.0	2.0876E+00	
44	1.9880E+00	0.0	1.1651E-01	0.0	2.1044E+00	
45	1.9896E+00	0.0	1.2309E-01	0.0	2.1128E+00	
46	1.9910E+00	0.0	1.3625E-01	0.0	2.1278E+00	
47	1.9909E+00	0.0	1.3969E-01	0.0	2.1308E+00	
48	1.9710E+00	0.0	1.3668E-01	0.0	2.1077E+00	
49	1.9240E+00	0.0	1.3344E-01	0.0	2.0574E+00	
50	1.8603E+00	0.0	1.3202E-01	0.0	1.9921E+00	

Fig. 4.5 Sample output of the DDXLIBMK code (Dump of DDX in a PDS file).

ANGLE NO	UPPER		LOWER		WIDTH
	COSINE	SINE	COSINE	SINE	
1	1.00000E+00	0.00000E+00	9.00000E-01	1.00000E-01	1.00000E-01
2	9.00000E-01	8.00000E-01	8.00000E-01	9.00000E-01	1.00000E-01
3	8.00000E-01	7.00000E-01	7.00000E-01	8.00000E-01	1.00000E-01
4	7.00000E-01	6.00000E-01	6.00000E-01	7.00000E-01	1.00000E-01
5	6.00000E-01	5.00000E-01	5.00000E-01	6.00000E-01	1.00000E-01
6	5.00000E-01	4.00000E-01	4.00000E-01	5.00000E-01	1.00000E-01
7	4.00000E-01	3.00000E-01	3.00000E-01	4.00000E-01	1.00000E-01
8	3.00000E-01	2.00000E-01	2.00000E-01	3.00000E-01	1.00000E-01
9	2.00000E-01	1.00000E-01	1.00000E-01	2.00000E-01	1.00000E-01
10	1.00000E-01	0.0	0.0	1.00000E-01	1.00000E-01
11	0.0	-1.00000E-01	-1.00000E-01	0.0	1.00000E-01
12	-1.00000E-01	-2.00000E-01	-2.00000E-01	-1.00000E-01	1.00000E-01
13	-2.00000E-01	-3.00000E-01	-3.00000E-01	-2.00000E-01	1.00000E-01
14	-3.00000E-01	-4.00000E-01	-4.00000E-01	-3.00000E-01	1.00000E-01
15	-4.00000E-01	-5.00000E-01	-5.00000E-01	-4.00000E-01	1.00000E-01
16	-5.00000E-01	-6.00000E-01	-6.00000E-01	-5.00000E-01	1.00000E-01
17	-6.00000E-01	-7.00000E-01	-7.00000E-01	-6.00000E-01	1.00000E-01
18	-7.00000E-01	-8.00000E-01	-8.00000E-01	-7.00000E-01	1.00000E-01
19	-8.00000E-01	-9.00000E-01	-9.00000E-01	-8.00000E-01	1.00000E-01
20	-9.00000E-01	-1.00000E+00	-1.00000E+00	-9.00000E-01	1.00000E-01
AT MAIN	B40306CT				
E-INCDNT	1	11	21	31	41
					125
					124
					121
					111
					101
					111
					124

**** SUFFIX OF VARIABLE DIMENSION ****

K01	K02	K03	K04	K05	K06	K07	K08	KLT
1	126	251	376	501	626	751	3251125750	
AT FILED	B40306CT							
AT FILED	B40306TA							

Fig. 4.5 (continued)

***** MATNO = 306 *****

MULTI-GROUP CROSS SECTION

GROUP	PRODUCTION	FISSION	CAPTURE	NU-FISSION	TOTAL
101	7.3212E-01	0.0	1.8972E+00	0.0	2.6293E+00
102	7.3258E-01	0.0	2.1459E+00	0.0	2.8784E+00
103	7.3296E-01	0.0	2.4284E+00	0.0	3.1614E+00
104	7.3328E-01	0.0	2.7494E+00	0.0	3.4826E+00
105	7.3355E-01	0.0	3.1136E+00	0.0	3.8471E+00
106	7.3376E-01	0.0	3.5269E+00	0.0	4.2607E+00
107	7.3393E-01	0.0	3.9958E+00	0.0	4.7297E+00
108	7.3410E-01	0.0	4.5272E+00	0.0	5.2613E+00
109	7.3424E-01	0.0	5.4717E+00	0.0	6.2059E+00
110	7.3437E-01	0.0	7.0271E+00	0.0	7.7614E+00
111	7.3449E-01	0.0	9.0245E+00	0.0	9.7590E+00
112	7.3462E-01	0.0	1.1590E+01	0.0	1.2324E+01
113	7.3473E-01	0.0	1.4884E+01	0.0	1.5619E+01
114	7.3481E-01	0.0	1.9115E+01	0.0	1.9849E+01
115	7.3487E-01	0.0	2.4547E+01	0.0	2.5282E+01
116	7.3493E-01	0.0	3.1524E+01	0.0	3.2259E+01
117	7.3499E-01	0.0	4.0484E+01	0.0	4.1219E+01
118	7.3516E-01	0.0	5.1988E+01	0.0	5.2723E+01
119	7.3547E-01	0.0	6.6758E+01	0.0	6.7494E+01
120	7.3579E-01	0.0	8.5724E+01	0.0	8.6459E+01
121	7.3611E-01	0.0	1.1008E+02	0.0	1.1081E+02
122	7.3679E-01	0.0	1.4135E+02	0.0	1.4209E+02
123	7.3886E-01	0.0	1.8150E+02	0.0	1.8224E+02
124	7.4196E-01	0.0	2.3306E+02	0.0	2.3380E+02
125	7.9962E-01	0.0	8.2142E+02	0.0	8.2222E+02
AT FILED B40306TB					

OUTPUT OF DDX LIBRARY

SOURCE GROUP= 1 MAXSD=125 UPPER= 1.64870E+07 LOWER= 1.62314E+07

SLOWING DOWN GROUP NUMBER

MU	1	2	3	4	5	6	7	8	9	10
1	8.762E-02	1.379E-01	6.646E-02	1.177E-03	1.154E-06	2.867E-06	4.515E-06	6.348E-06	9.960E-06	7.944E-04
2	0.0	0.0	3.013E-02	6.717E-02	3.801E-02	1.916E-03	4.258E-06	5.986E-06	9.392E-06	1.457E-05
3	0.0	0.0	0.0	1.763E-08	9.147E-03	3.031E-02	2.026E-02	2.247E-03	8.786E-06	1.363E-05
4	0.0	0.0	0.0	1.658E-08	9.581E-07	2.380E-06	2.413E-03	1.331E-02	9.964E-03	1.948E-03
5	0.0	0.0	0.0	1.563E-08	9.028E-07	2.422E-06	3.513E-06	4.964E-06	5.079E-04	5.542E-03
6	0.0	0.0	0.0	1.468E-08	8.479E-07	2.106E-06	3.317E-06	4.662E-06	7.316E-06	1.135E-05
7	0.0	0.0	0.0	1.381E-08	7.981E-07	1.982E-06	3.122E-06	4.388E-06	6.886E-06	1.068E-05
8	0.0	0.0	0.0	1.294E-08	7.479E-07	1.857E-06	2.925E-06	4.112E-06	6.452E-06	1.001E-05
9	0.0	0.0	0.0	1.217E-08	7.033E-07	1.747E-06	2.751E-06	3.867E-06	6.068E-06	9.411E-06
10	0.0	0.0	0.0	1.141E-08	6.595E-07	1.638E-06	2.580E-06	3.626E-06	5.690E-06	8.825E-06
11	0.0	0.0	0.0	1.073E-08	6.199E-07	1.540E-06	2.425E-06	3.409E-06	5.349E-06	8.295E-06
12	0.0	0.0	0.0	1.009E-08	5.832E-07	1.448E-06	2.281E-06	3.207E-06	5.032E-06	7.804E-06
13	0.0	0.0	0.0	9.485E-09	5.480E-07	1.361E-06	2.143E-06	3.013E-06	4.728E-06	7.333E-06
14	0.0	0.0	0.0	8.972E-09	5.184E-07	1.287E-06	2.028E-06	2.850E-06	4.472E-06	6.936E-06
15	0.0	0.0	0.0	8.426E-09	4.869E-07	1.209E-06	1.904E-06	2.677E-06	4.201E-06	6.515E-06
16	0.0	0.0	0.0	7.943E-09	4.589E-07	1.140E-06	1.795E-06	2.524E-06	3.960E-06	6.141E-06
17	0.0	0.0	0.0	7.449E-09	4.304E-07	1.069E-06	1.683E-06	2.366E-06	3.713E-06	5.759E-06
18	0.0	0.0	0.0	7.003E-09	4.046E-07	1.005E-06	1.583E-06	2.225E-06	3.491E-06	5.414E-06
19	0.0	0.0	0.0	6.635E-09	3.834E-07	9.521E-07	1.499E-06	2.108E-06	3.308E-06	5.130E-06
20	0.0	0.0	0.0	6.219E-09	3.593E-07	8.924E-07	1.405E-06	2.000E-06	3.100E-06	4.808E-06

Fig. 4.5 (continued)

***** MATNO = 306 *****

GROUP	PRODUCTION	FISSION	MULTI-GROUP CROSS SECTION		TOTAL
			CAPTURE	NU-FISSION	
101	7.3212E-01	0.0	1.8972E+00	0.0	2.6293E+00
102	7.3258E-01	0.0	2.1459E+00	0.0	2.8784E+00
103	7.3296E-01	0.0	2.4284E+00	0.0	3.1614E+00
104	7.3328E-01	0.0	2.7494E+00	0.0	3.4826E+00
105	7.3355E-01	0.0	3.1136E+00	0.0	3.8471E+00
106	7.3376E-01	0.0	3.5269E+00	0.0	4.2607E+00
107	7.3393E-01	0.0	3.9958E+00	0.0	4.7297E+00
108	7.3410E-01	0.0	4.5272E+00	0.0	5.2613E+00
109	7.3424E-01	0.0	5.4717E+00	0.0	6.2059E+00
110	7.3437E-01	0.0	7.0271E+00	0.0	7.7614E+00
111	7.3449E-01	0.0	9.0245E+00	0.0	9.7590E+00
112	7.3462E-01	0.0	1.1590E+01	0.0	1.2324E+01
113	7.3473E-01	0.0	1.4884E+01	0.0	1.5619E+01
114	7.3481E-01	0.0	1.9150E+01	0.0	1.9849E+01
115	7.3487E-01	0.0	2.4547E+01	0.0	2.5282E+01
116	7.3493E-01	0.0	3.1524E+01	0.0	3.2259E+01
117	7.3499E-01	0.0	4.0484E+01	0.0	4.1219E+01
118	7.3516E-01	0.0	5.1988E+01	0.0	5.2723E+01
119	7.3547E-01	0.0	6.6750E+01	0.0	6.7494E+01
120	7.3579E-01	0.0	8.5724E+01	0.0	8.6459E+01
121	7.3611E-01	0.0	1.1008E+02	0.0	1.1081E+02
122	7.3679E-01	0.0	1.4135E+02	0.0	1.4209E+02
123	7.3886E-01	0.0	1.8150E+02	0.0	1.8224E+02
124	7.4196E-01	0.0	2.3300E+02	0.0	2.3380E+02
125	7.9622E-01	0.0	8.2142E+02	0.0	8.2222E+02

AT FILED B40306TB

OUTPUT OF DDX LIBRARY

SOURCE GROUP= 1 MAXSD=125 EUPPER= 1.64870E+07 ELOWER= 1.62314E+07 SLOWING DOWN GROUP NUMBER

MU	1	2	3	4	5	6	7	8	9	10
1	8.762E-02	1.379E-01	6.646E-02	1.177E-03	1.154E-05	2.867E-06	4.515E-06	6.348E-06	9.960E-06	7.944E-05
2	0.0	0.0	3.013E-02	6.717E-02	3.801E-02	1.916E-03	4.258E-06	5.986E-06	9.392E-06	1.457E-05
3	0.0	0.0	0.0	1.763E-08	9.147E-03	3.031E-02	2.026E-02	2.247E-03	8.786E-06	1.363E-05
4	0.0	0.0	0.0	1.658E-08	9.581E-07	2.380E-06	2.413E-03	1.331E-02	9.964E-03	1.948E-03
5	0.0	0.0	0.0	1.563E-08	9.028E-07	2.242E-06	3.531E-06	5.079E-04	5.542E-03	1.135E-05
6	0.0	0.0	0.0	1.4668E-08	8.479E-07	2.106E-06	3.317E-06	4.6662E-06	7.316E-06	8.886E-06
7	0.0	0.0	0.0	1.381E-08	7.981E-07	1.982E-06	3.122E-06	4.388E-06	6.8295E-06	1.068E-05
8	0.0	0.0	0.0	1.294E-08	7.479E-07	1.857E-06	2.925E-06	4.112E-06	6.452E-06	1.001E-05
9	0.0	0.0	0.0	1.217E-08	7.033E-07	1.747E-06	2.751E-06	3.867E-06	6.068E-06	9.411E-06
10	0.0	0.0	0.0	1.141E-08	6.595E-07	1.638E-06	2.580E-06	3.626E-06	8.825E-06	1.201E-06
11	0.0	0.0	0.0	1.073E-08	6.199E-07	1.540E-06	2.425E-06	3.409E-06	5.349E-06	8.295E-06
12	0.0	0.0	0.0	1.009E-08	5.832E-07	1.448E-06	2.281E-06	3.207E-06	5.032E-06	7.804E-06
13	0.0	0.0	0.0	9.485E-09	5.480E-07	1.361E-06	2.143E-06	3.013E-06	4.728E-06	7.333E-06
14	0.0	0.0	0.0	8.972E-09	5.184E-07	1.287E-06	2.028E-06	2.850E-06	4.472E-06	6.936E-06
15	0.0	0.0	0.0	8.4226E-09	4.869E-07	1.209E-06	1.904E-06	2.677E-06	4.201E-06	6.515E-06
16	0.0	0.0	0.0	7.943E-09	4.589E-07	1.140E-06	1.795E-06	2.524E-06	3.960E-06	6.141E-06
17	0.0	0.0	0.0	7.449E-09	4.304E-07	1.069E-06	1.683E-06	2.366E-06	3.713E-06	5.759E-06
18	0.0	0.0	0.0	7.003E-09	4.046E-07	1.005E-06	1.583E-06	2.225E-06	3.491E-06	5.414E-06
19	0.0	0.0	0.0	6.6335E-09	3.834E-07	9.521E-07	1.499E-06	2.108E-06	3.308E-06	5.130E-06
20	0.0	0.0	0.0	6.219E-09	3.593E-07	8.924E-07	1.405E-06	1.976E-06	3.100E-06	4.808E-06

MU 11 12 13 14 15 16 17 18 19 20

Fig. 4.5 (continued)

1	2-304E-03	5.442E-04	3.961E-05	4.627E-05	5.434E-05	7.653E-05	9.619E-05	9.836E-05	8.724E-05
2	1.958E-05	2.234E-04	1.696E-03	2.113E-03	6.875E-04	5.064E-05	5.834E-05	6.566E-05	7.758E-05
3	1.831E-05	2.306E-05	2.915E-05	2.170E-05	2.743E-05	3.287E-05	1.191E-03	2.015E-03	1.019E-04
4	1.723E-05	5.203E-03	1.419E-03	2.584E-05	3.098E-05	3.619E-05	4.452E-05	4.452E-05	7.475E-05
5	5.203E-03	8.855E-05	2.389E-03	2.941E-03	1.232E-03	3.398E-05	4.200E-05	4.839E-05	1.396E-03
6	7.1435E-05	1.049E-05	1.807E-05	2.285E-05	1.206E-03	2.068E-03	3.945E-05	4.544E-05	6.224E-05
7	8.199E-05	1.321E-05	1.693E-05	2.141E-05	2.566E-05	2.141E-05	1.822E-03	1.237E-03	5.858E-05
8	9.1265E-05	1.265E-05	1.593E-05	2.013E-05	2.413E-05	2.819E-05	2.722E-05	3.669E-05	5.489E-05
9	1.186E-05	1.115E-05	1.493E-05	1.888E-05	2.263E-05	2.643E-05	3.068E-05	3.534E-05	1.559E-05
10	1.253E-06	1.040E-05	1.774E-05	2.127E-05	2.485E-05	2.884E-05	2.135E-05	2.609E-05	4.404E-05
11	1.314E-06	1.039E-05	1.39E-05	1.755E-05	1.839E-05	1.951E-05	2.177E-05	2.936E-05	2.866E-04
12	1.385E-06	1.241E-05	1.669E-05	2.001E-05	2.337E-05	2.713E-05	2.002E-05	2.322E-05	4.140E-05
13	1.456E-06	1.262E-05	1.569E-05	1.880E-05	2.196E-05	2.549E-05	2.937E-05	3.518E-05	4.281E-05
14	1.522E-06	1.174E-05	1.484E-05	1.778E-05	2.078E-05	2.411E-05	2.411E-05	2.778E-05	3.122E-05
15	1.595E-06	1.102E-05	1.394E-05	1.670E-05	1.951E-05	2.265E-05	2.135E-05	2.609E-05	3.251E-05
16	1.664E-06	1.039E-05	1.314E-05	1.575E-05	1.839E-05	2.177E-05	2.002E-05	2.460E-05	3.065E-05
17	1.739E-06	9.745E-06	1.232E-05	1.477E-05	1.725E-05	2.002E-05	2.306E-05	2.596E-05	3.159E-05
18	1.811E-06	1.158E-06	1.880E-05	1.622E-05	1.880E-05	1.622E-05	1.688E-05	2.168E-05	2.970E-05
19	1.884E-06	8.681E-06	1.097E-05	1.315E-05	1.536E-05	1.783E-05	2.054E-05	2.312E-05	2.560E-05
20	1.946E-06	8.136E-06	1.029E-05	1.233E-05	1.440E-05	1.672E-05	1.926E-05	2.167E-05	2.814E-05
MU	21	9.207E-05	9.898E-05	1.056E-04	1.129E-04	1.187E-04	1.263E-04	1.338E-04	1.480E-04
	22	8.239E-05	1.027E-04	9.959E-05	1.065E-04	1.120E-04	1.191E-04	1.262E-04	1.468E-04
	23	7.641E-05	8.216E-05	1.178E-04	1.193E-04	1.094E-04	1.114E-04	1.235E-04	1.373E-04
	24	7.485E-03	9.897E-04	8.259E-05	8.831E-05	9.286E-05	9.983E-05	1.199E-04	1.227E-04
	25	6.742E-05	5.743E-04	1.424E-03	1.028E-03	1.037E-04	9.820E-05	1.177E-04	1.321E-04
	26	7.365E-05	6.843E-05	7.301E-05	5.617E-04	1.250E-03	1.154E-03	6.135E-04	1.020E-04
	27	6.964E-05	6.413E-05	6.842E-05	7.315E-05	7.692E-05	8.177E-05	7.380E-05	1.073E-04
	28	6.528E-04	6.031E-05	6.434E-05	6.880E-05	7.233E-05	7.689E-05	8.140E-05	1.055E-04
	29	6.1587E-03	1.615E-03	4.209E-04	6.451E-05	6.783E-05	7.209E-05	7.631E-05	1.073E-03
	30	5.944E-05	1.577E-04	1.363E-03	1.656E-03	1.380E-04	6.776E-05	7.172E-05	8.857E-05
	31	5.651E-05	5.001E-05	5.335E-05	7.644E-05	9.987E-04	1.541E-03	8.149E-04	7.498E-05
	32	4.371E-05	4.699E-05	5.013E-05	5.361E-05	5.633E-05	5.989E-05	7.101E-04	7.443E-05
	33	4.134E-05	4.445E-05	4.742E-05	5.071E-05	5.331E-05	5.664E-05	6.993E-05	6.264E-05
	34	3.883E-05	4.175E-05	4.454E-05	4.762E-05	5.007E-05	5.319E-05	5.628E-05	6.522E-05
	35	3.660E-05	3.935E-05	4.199E-05	4.489E-05	4.720E-05	5.013E-05	5.304E-05	5.543E-05
	36	3.432E-05	3.690E-05	3.937E-05	4.210E-05	4.426E-05	4.720E-05	4.973E-05	5.196E-05
	37	3.227E-05	3.470E-05	3.702E-05	3.958E-05	4.161E-05	4.419E-05	4.675E-05	4.888E-05
	38	3.057E-05	3.287E-05	3.507E-05	3.750E-05	3.942E-05	4.186E-05	4.427E-05	4.626E-05
	39	2.866E-05	3.081E-05	3.287E-05	3.515E-05	3.695E-05	4.150E-05	4.335E-05	4.573E-05
MU	40	1.624E-04	1.707E-04	7.705E-04	9.092E-04	9.092E-04	1.036E-03	1.235E-03	1.342E-03
	41	1.531E-04	1.608E-04	7.256E-04	8.556E-04	9.743E-04	1.077E-03	1.161E-03	1.251E-03
	42	1.431E-04	1.503E-04	6.781E-04	7.991E-04	9.096E-04	1.005E-03	1.083E-03	1.166E-03
	43	1.346E-04	1.413E-04	6.368E-04	7.496E-04	8.525E-04	9.415E-04	1.014E-03	1.091E-03
	44	1.267E-04	1.330E-04	5.989E-04	7.024E-04	8.002E-04	8.831E-04	9.502E-04	1.021E-03
	45	1.196E-04	1.341E-04	5.618E-04	6.603E-04	7.499E-04	8.272E-04	8.898E-04	9.319E-04
	46	1.118E-04	1.294E-04	5.718E-04	6.200E-04	7.036E-04	7.758E-04	8.340E-04	8.732E-04
	47	1.047E-04	1.099E-04	5.296E-04	5.901E-04	6.574E-04	7.244E-04	7.785E-04	8.147E-04
	48	9.941E-04	7.124E-04	4.640E-04	5.956E-04	6.167E-04	6.792E-04	7.296E-04	7.820E-04
	49	8.738E-04	7.409E-04	5.595E-04	5.225E-04	6.059E-04	6.394E-04	6.818E-04	7.130E-04
	50	8.667E-05	9.085E-05	2.122E-03	4.776E-04	5.800E-04	5.966E-04	6.385E-04	6.676E-04
	51	8.149E-05	8.540E-05	7.178E-04	1.920E-03	5.107E-04	6.006E-04	5.987E-04	6.257E-04
	52	7.653E-05	8.018E-05	3.597E-04	1.595E-03	7.021E-04	5.449E-04	5.763E-04	5.992E-04
	53	8.869E-04	1.383E-04	3.397E-04	4.242E-04	1.903E-03	4.923E-04	5.694E-04	5.518E-04
	54	8.178E-04	1.176E-04	3.716E-04	4.095E-04	5.225E-04	6.394E-04	6.818E-04	7.334E-04
	55	8.697E-05	6.697E-05	1.806E-03	4.776E-04	5.800E-04	5.966E-04	6.385E-04	6.834E-04
	56	8.276E-05	5.947E-04	3.497E-04	1.920E-03	5.107E-04	6.006E-04	5.987E-04	6.404E-04
	57	7.653E-05	5.036E-04	3.597E-04	4.242E-04	1.903E-03	4.923E-04	5.694E-04	5.518E-04
	58	7.1435E-05	4.009E-04	3.397E-04	4.095E-04	5.225E-04	6.394E-04	6.818E-04	7.334E-04
	59	6.634E-05	3.009E-04	3.716E-04	4.095E-04	5.225E-04	6.394E-04	6.818E-04	7.334E-04
	60	6.1332E-05	2.009E-04	3.497E-04	3.497E-04	3.497E-04	3.497E-04	3.497E-04	3.497E-04

Fig. 4.5 (continued)

SOURCE GROUP=124		MAXSD= 2	UPPER= 5.31565E-01	ELOWER= 3.22411E-01	SLOWING DOWN GROUP NUMBER
MU					
1	6.455E-02	2.354E-02			
2	5.874E-02	6.709E-03			
3	5.252E-02	1.075E-02			
4	4.666E-02	1.450E-02			
5	4.104E-02	1.809E-02			
6	3.583E-02	2.133E-02			
7	3.094E-02	2.431E-02			
8	2.626E-02	2.715E-02			
9	2.188E-02	2.976E-02			
10	1.782E-02	3.210E-02			
11	1.422E-02	3.510E-02			
12	1.022E-02	3.639E-02			
13	6.874E-03	3.819E-02			
14	3.705E-03	3.985E-02			
15	8.316E-04	4.128E-02			
16	0.0	4.071E-02			
17	0.0	3.935E-02			
18	0.0	3.804E-02			
19	0.0	3.677E-02			
20	0.0	3.514E-02			

SOURCE GROUP=125		MAXSD= 1	UPPER= 3.22411E-01	ELOWER= 1.00100E-05	SLOWING DOWN GROUP NUMBER
MU					
1	5.000E-02	1			
2	5.000E-02				
3	5.000E-02				
4	5.000E-02				
5	5.000E-02				
6	5.000E-02				
7	5.000E-02				
8	5.000E-02				
9	5.000E-02				
10	5.000E-02				
11	5.000E-02				
12	5.000E-02				
13	5.000E-02				
14	5.000E-02				
15	5.000E-02				
16	5.000E-02				
17	5.000E-02				
18	5.000E-02				
19	5.000E-02				
20	5.000E-02				

Fig. 4.5 (continued)

5. Concluding Remarks

The PROF-DD code system has been developed for fusion neutronics calculations. This system generates a multi-group double-differential form cross section (DDX) library by processing the nuclear data files compiled with the ENDF/B format. A user can generate a multi-group DDX library by using this system with a few input data within a moderate computation time. This report gives a user how to use this system for generating a DDX library. The produced DDX library by this system can be used in the Monte Carlo code MORSE-DD, 1- and 2-dimensional Sn transport codes ANISN-DD and DOT-DD. The validity of the produced library was examined through extensive benchmark calculations and was found to be satisfactory as compared with a continuous energy Monte Carlo method. These results are described in Reference (3).

Acknowledgments

The authors wish to express their thanks to Messrs. Y. Matsui and K. Kaneko of Japan Information Service Co. Ltd. for their assistance in programming.

5. Concluding Remarks

The PROF-DD code system has been developed for fusion neutronics calculations. This system generates a multi-group double-differential form cross section (DDX) library by processing the nuclear data files compiled with the ENDF/B format. A user can generate a multi-group DDX library by using this system with a few input data within a moderate computation time. This report gives a user how to use this system for generating a DDX library. The produced DDX library by this system can be used in the Monte Carlo code MORSE-DD, 1- and 2-dimensional Sn transport codes ANISN-DD and DOT-DD. The validity of the produced library was examined through extensive benchmark calculations and was found to be satisfactory as compared with a continuous energy Monte Carlo method. These results are described in Reference (3).

Acknowledgments

The authors wish to express their thanks to Messrs. Y. Matsui and K. Kaneko of Japan Information Service Co. Ltd. for their assistance in programming.

References

- 1) Takahashi, A. and Rusch, D.: 'Fast Rigorous Numerical Method for the Solution of the Anisotropic Neutron Transport Problem and the NITRUN System for Fusion Neutronics Applications', KfK 2832/1,2 (1979).
- 2) Nakagawa, M. and Mori, T.: 'MORSE-DD: A Monté Carlo Code Using Multi-Group Double-Differential Form Cross Sections', JAERI-M 84-126 (1984).
- 3) Nakagawa, M., Mori, T. and Ishiguro, Y.: 'Benchmark Test of MORSE-DD Code using Double-Differential Form Cross Sections', JAERI-M 85-009 (1985) (in Japanese).
- 4) Mori, T. and Nakagawa, M.: to be published.
- 5) Drake, M.K. (ed.): 'Data Formats and Procedures For the ENDF Neutron Cross Section Library', BNL 50274(T-601), ENDF 102, Vol.1 (1970).
- 6) Nakagawa, T.: 'Program RESEND (Version 84-07): A Program for Reconstruction of Resonance Cross Sections from Evaluated Nuclear Data in the ENDF/B Format', JAERI-M 84-192 (1984).
- 7) Hasegawa, A.; private communication (1984).
Detailed descriptions are given in UCRL-50400, Vol.17 Part A-C by D.E. Cullen (1979).
- 8) Takano, H., Hasegawa, A. and Kaneko, K.: 'TIMS-PGG: A Code System for Producing Group Constants in Fast Neutron Energy Region', JAERI-M 82-072 (1982).

Appendix Available DDX libraries

A.1 DDXLIB1 and DDXLIB3 Libraries

DDXLIB1 and DDXLIB3 libraries have been produced with the same energy group and angle mesh structures from the nuclear data, ENDF/B-IV and JENDL-3PR1. They contain the same elements. The energy group structure and ID number of each element are shown in Tables A.1 and A.2, respectively. The 20 equi-cosine bins are employed in both libraries.

The parameters for the DDXLIB1 library are as follows:

NO40= 0: 124-group library with slowing down probability to the 125-th group,

IUP2= 1: collision density is assumed to be constant in lethargy within each group,

IF45= 1: isotropic scattering is assumed for reaction for which kinematics are not known,

EPSPR : 10^{-5} ,

Weighting function : $1/E$.

In this library, the cross section for each reaction is assumed to be 0.0 in a energy group which includes the threshold energy for this reaction. The MORSE-DD calculations with this library have shown a good prediction accuracy in various applications³⁾.

The DDXLIB3 library has been newly produced with the following parameters:

NO40=-1: 125-group library with slowing down probability to the 125-th group,

IUP2= 2: collision density is $\sigma(E^*)\Psi_w(E^*)$,

IF45= 2: angular dependence is taken from File 4 for reaction for which kinematics are not known,

EPSPR : 10^{-10} ,

Weighting function : Maxwellian < 0.32 eV,
 $1/E > 0.32$ eV.

For processing the Beryllium data in both libraries, the LINEAR and SIGMA1 codes have been used in place of the RESEND code. These two libraries and their master files are stored on the magnetic disk with the following names.

DDX library Master file

DDXLIB1 : J3803.DDXLIB1.DATA J3803.PROFDDX.PDS124G.DATA (B-4)
 J3803.DDXLIB2.DATA J3803.PROFDDX2.PDS124G.DATA (J-3)
 DDXLIB3 : J3803.DDXLIB3.DATA J3803.DDXLIB3.PDS125G.DATA

A.2 Comparison between DDXLIB1 and DDXLIB3 Libraries

Angle-integrated energy distributions from oxygen are compared in Fig. A.1 between DDXLIB1 and DDXLIB3 libraries. The data of DDXLIB1 are not observed in a lower energy region, which is ascribed to that the DDXLIB1 neglects the scattering in the vicinities of threshold energies and those with probability less than 1×10^{-5} . As for the other elements, however, this discrepancy was not found. Figure 4.3-(b) shows the DDX of lithium-7 in the direction of $\mu = -0.65$. The difference between the DDXLIB1 and the DDXLIB3 in the smooth part of distribution is due to the difference of IF45, i.e. the difference of treatment of angular distribution of reactions like continuum inelastic scattering. Consequently, energy-integrated angle distributions are considerably different from each other, as seen in Fig. 4.3-(c). The DDXLIB3 shows generally good agreement with the DDXLIB4, which is calculated by processing double-differential data in File 6. There is no difference in angle-integrated energy distribution, as seen in Fig. 4.3-(a). As a result, there are large discrepancies among leakage spectra calculated from these libraries, as shown in Fig. A.2 in the case of a 20 cm thick lithium slab. Leakage flux predicted from the DDXLIB3 is slightly higher than that from the DDXLIB1. On the other hand, no large difference is observed in the calculated spectra in the $\text{Li}_2\text{O}-\text{C}$ sphere, as shown in Fig. A.3. In this system, calculated reaction rates for ${}^7\text{Li}(n,n'\alpha)$ and ${}^6\text{Li}(n,\alpha)$ agree with each other within 1 % and 3 %, respectively. In this case, the calculated flux from the DDXLIB3 becomes slightly higher than that from the DDXLIB1 as the distance from the center of the sphere becomes larger.

The discrepancies owing to the difference of IUP2 are not observed except for nuclides with large resonances such as

iron. They are shown in Fig. A.4, which shows leakage spectra from a 10 cm thick stainless steel slab calculated with these two libraries.

Table A.1 Energy group structure of DDXLIB1 and DDXLIB3 libraries

GROUP	ENERGY RANGE	LETHARGY RANGE	GROUP	ENERGY RANGE	LETHARGY RANGE
1	1.6231E+07 - 1.6487E+07	-0.500 - -0.484	64	1.0540E+06 - 1.1943E+06	2.125 - 2.250
2	1.5980E+07 - 1.6231E+07	-0.484 - -0.469	65	9.3013E+05 - 1.0540E+06	2.250 - 2.375
3	1.5732E+07 - 1.5980E+07	-0.469 - -0.453	66	8.2083E+05 - 9.3013E+05	2.375 - 2.500
4	1.5488E+07 - 1.5732E+07	-0.453 - -0.437	67	7.2438E+05 - 8.2083E+05	2.500 - 2.625
5	1.5248E+07 - 1.5488E+07	-0.437 - -0.422	68	6.3927E+05 - 7.2438E+05	2.625 - 2.750
6	1.5012E+07 - 1.5248E+07	-0.422 - -0.406	69	5.6415E+05 - 6.3927E+05	2.750 - 2.875
7	1.4779E+07 - 1.5012E+07	-0.406 - -0.391	70	4.9786E+05 - 5.6415E+05	2.875 - 3.000
8	1.4550E+07 - 1.4779E+07	-0.391 - -0.375	71	4.3936E+05 - 4.9786E+05	3.000 - 3.125
9	1.4324E+07 - 1.4550E+07	-0.375 - -0.359	72	3.8773E+05 - 4.3936E+05	3.125 - 3.250
10	1.4102E+07 - 1.4324E+07	-0.359 - -0.344	73	3.4217E+05 - 3.8773E+05	3.250 - 3.375
11	1.3883E+07 - 1.4102E+07	-0.344 - -0.328	74	3.0197E+05 - 3.4217E+05	3.375 - 3.500
12	1.3668E+07 - 1.3883E+07	-0.328 - -0.312	75	2.6649E+05 - 3.0197E+05	3.500 - 3.625
13	1.3456E+07 - 1.3668E+07	-0.312 - -0.297	76	2.3517E+05 - 2.6649E+05	3.625 - 3.750
14	1.3248E+07 - 1.3456E+07	-0.297 - -0.281	77	2.0754E+05 - 2.3517E+05	3.750 - 3.875
15	1.3042E+07 - 1.3248E+07	-0.281 - -0.266	78	1.8315E+05 - 2.0754E+05	3.875 - 4.000
16	1.2840E+07 - 1.3042E+07	-0.266 - -0.250	79	1.6163E+05 - 1.8315E+05	4.000 - 4.125
17	1.2641E+07 - 1.2840E+07	-0.250 - -0.234	80	1.4264E+05 - 1.6163E+05	4.125 - 4.250
18	1.2445E+07 - 1.2641E+07	-0.234 - -0.219	81	1.2588E+05 - 1.4264E+05	4.250 - 4.375
19	1.2252E+07 - 1.2445E+07	-0.219 - -0.203	82	1.1109E+05 - 1.2588E+05	4.375 - 4.500
20	1.2062E+07 - 1.2252E+07	-0.203 - -0.187	83	9.8035E+04 - 1.1109E+05	4.500 - 4.625
21	1.1875E+07 - 1.2062E+07	-0.187 - -0.172	84	8.6515E+04 - 9.8035E+04	4.625 - 4.750
22	1.1691E+07 - 1.1875E+07	-0.172 - -0.156	85	7.6349E+04 - 8.6515E+04	4.750 - 4.875
23	1.1510E+07 - 1.1691E+07	-0.156 - -0.141	86	6.7378E+04 - 7.6349E+04	4.875 - 5.000
24	1.1331E+07 - 1.1510E+07	-0.141 - -0.125	87	5.9461E+04 - 6.7378E+04	5.000 - 5.125
25	1.1156E+07 - 1.1331E+07	-0.125 - -0.109	88	5.2474E+04 - 5.9461E+04	5.125 - 5.250
26	1.0983E+07 - 1.1156E+07	-0.109 - -0.094	89	4.6308E+04 - 5.2474E+04	5.250 - 5.375
27	1.0812E+07 - 1.0983E+07	-0.094 - -0.078	90	4.0867E+04 - 4.6308E+04	5.375 - 5.500
28	1.0645E+07 - 1.0812E+07	-0.078 - -0.063	91	3.6065E+04 - 4.0867E+04	5.500 - 5.625
29	1.0480E+07 - 1.0645E+07	-0.063 - -0.047	92	3.1827E+04 - 3.6065E+04	5.625 - 5.750
30	1.0317E+07 - 1.0480E+07	-0.047 - -0.031	93	2.8087E+04 - 3.1827E+04	5.750 - 5.875
31	1.0157E+07 - 1.0317E+07	-0.031 - -0.016	94	2.4787E+04 - 2.8087E+04	5.875 - 6.000
32	9.9999E+06 - 1.0157E+07	-0.016 - 0.000	95	2.1874E+04 - 2.4787E+04	6.000 - 6.125
33	9.3940E+06 - 9.9999E+06	0.000 - 0.063	96	1.9304E+04 - 2.1874E+04	6.125 - 6.250
34	8.8249E+06 - 9.3940E+06	0.063 - 0.125	97	1.5034E+04 - 1.9304E+04	6.250 - 6.500
35	8.2902E+06 - 8.8249E+06	0.125 - 0.188	98	1.1709E+04 - 1.5034E+04	6.500 - 6.750
36	7.7879E+06 - 8.2902E+06	0.188 - 0.250	99	9.1186E+03 - 1.1709E+04	6.750 - 7.000
37	7.3161E+06 - 7.7879E+06	0.250 - 0.313	100	7.1016E+03 - 9.1186E+03	7.000 - 7.250
38	6.8728E+06 - 7.3161E+06	0.313 - 0.375	101	5.5307E+03 - 7.1016E+03	7.250 - 7.500
39	6.4564E+06 - 6.8728E+06	0.375 - 0.438	102	4.3073E+03 - 5.5307E+03	7.500 - 7.750
40	6.0652E+06 - 6.4564E+06	0.438 - 0.500	103	3.3546E+03 - 4.3073E+03	7.750 - 8.000
41	5.6977E+06 - 6.0652E+06	0.500 - 0.563	104	2.6125E+03 - 3.3546E+03	8.000 - 8.250
42	5.3525E+06 - 5.6977E+06	0.563 - 0.625	105	2.0346E+03 - 2.6125E+03	8.250 - 8.500
43	5.0282E+06 - 5.3525E+06	0.625 - 0.688	106	1.5846E+03 - 2.0346E+03	8.500 - 8.750
44	4.7236E+06 - 5.0282E+06	0.688 - 0.750	107	1.2341E+03 - 1.5846E+03	8.750 - 9.000
45	4.4374E+06 - 4.7236E+06	0.750 - 0.813	108	9.6109E+02 - 1.2341E+03	9.000 - 9.250
46	4.1686E+06 - 4.4374E+06	0.813 - 0.875	109	5.8293E+02 - 9.6109E+02	9.250 - 9.750
47	3.9160E+06 - 4.1686E+06	0.875 - 0.938	110	3.5357E+02 - 5.8293E+02	9.750 - 10.250
48	3.6787E+06 - 3.9160E+06	0.938 - 1.000	111	2.1445E+02 - 3.5357E+02	10.250 - 10.750
49	3.4559E+06 - 3.6787E+06	1.000 - 1.063	112	1.3007E+02 - 2.1445E+02	10.750 - 11.250
50	3.2465E+06 - 3.4559E+06	1.063 - 1.125	113	7.8891E+01 - 1.3007E+02	11.250 - 11.750
51	3.0498E+06 - 3.2465E+06	1.125 - 1.188	114	4.7850E+01 - 7.8891E+01	11.750 - 12.250
52	2.8650E+06 - 3.0498E+06	1.188 - 1.250	115	2.9023E+01 - 4.7850E+01	12.250 - 12.750
53	2.6914E+06 - 2.8650E+06	1.250 - 1.313	116	1.7603E+01 - 2.9023E+01	12.750 - 13.250
54	2.5284E+06 - 2.6914E+06	1.313 - 1.375	117	1.0677E+01 - 1.7603E+01	13.250 - 13.750
55	2.3752E+06 - 2.5284E+06	1.375 - 1.438	118	6.4758E+00 - 1.0677E+01	13.750 - 14.250
56	2.2313E+06 - 2.3752E+06	1.438 - 1.500	119	3.9278E+00 - 6.4758E+00	14.250 - 14.750
57	2.0961E+06 - 2.2313E+06	1.500 - 1.563	120	2.3823E+00 - 3.9278E+00	14.750 - 15.250
58	1.9691E+06 - 2.0961E+06	1.563 - 1.625	121	1.4449E+00 - 2.3823E+00	15.250 - 15.750
59	1.8498E+06 - 1.9691E+06	1.625 - 1.688	122	8.7640E-01 - 1.4449E+00	15.750 - 16.250
60	1.7377E+06 - 1.8498E+06	1.688 - 1.750	123	5.3157E-01 - 8.7640E-01	16.250 - 16.750
61	1.5335E+06 - 1.7377E+06	1.750 - 1.875	124	3.2241E-01 - 5.3157E-01	16.750 - 17.250
62	1.3533E+06 - 1.5335E+06	1.875 - 2.000	125	1.0010E-05 - 3.2241E-01	17.250 - 27.630
63	1.1943E+06 - 1.3533E+06	2.000 - 2.125			

Table A.2 Identification number of elements in DDXLIB1 and
DDXLIB3 libraries

Element	ID number			Element	ID number	
	ENDF/B4	JENDL-3PR1			ENDF/B4	JENDL-3PR1
H	1269			Si	1194	
⁶ Li	1271	306		K	1150	
⁷ Li	1272	307		Ca	1195	
¹² C	1274	612		Cr	1191	2400
⁹ Be	1289	409		Fe	1192	2600
¹⁴ N	1275			Ni	1190	2800
¹⁶ O	1276	816		⁵⁵ Mn	1197	
²³ Na	1156			Cu	1295	
Mg	1280			Mo	1287	
²⁷ Al	1193			Pb	1288	

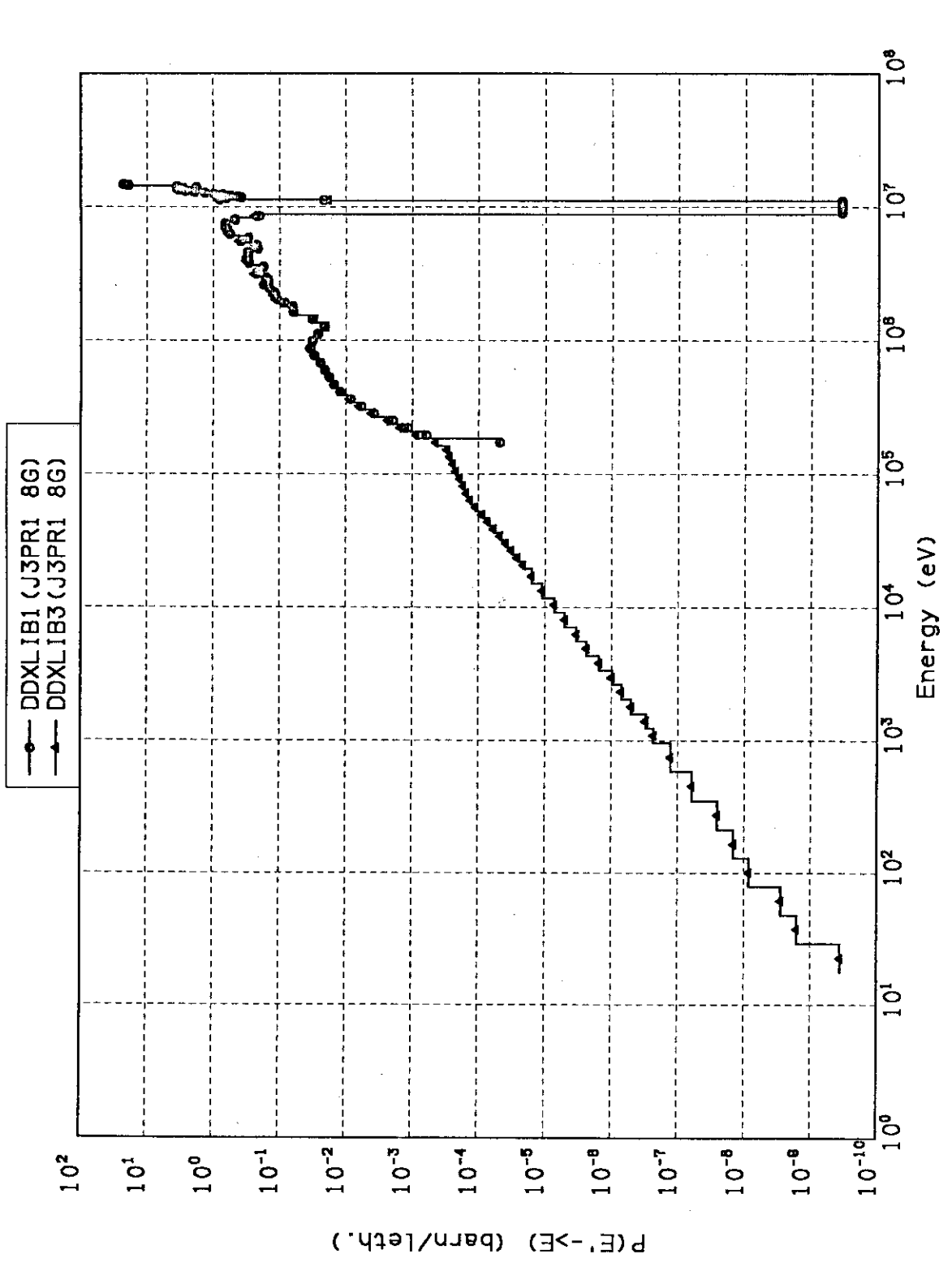


Fig.A.1 Comparison of energy distributions of scattered neutrons from oxygen between DDXLIB1 and DDXLIB3.

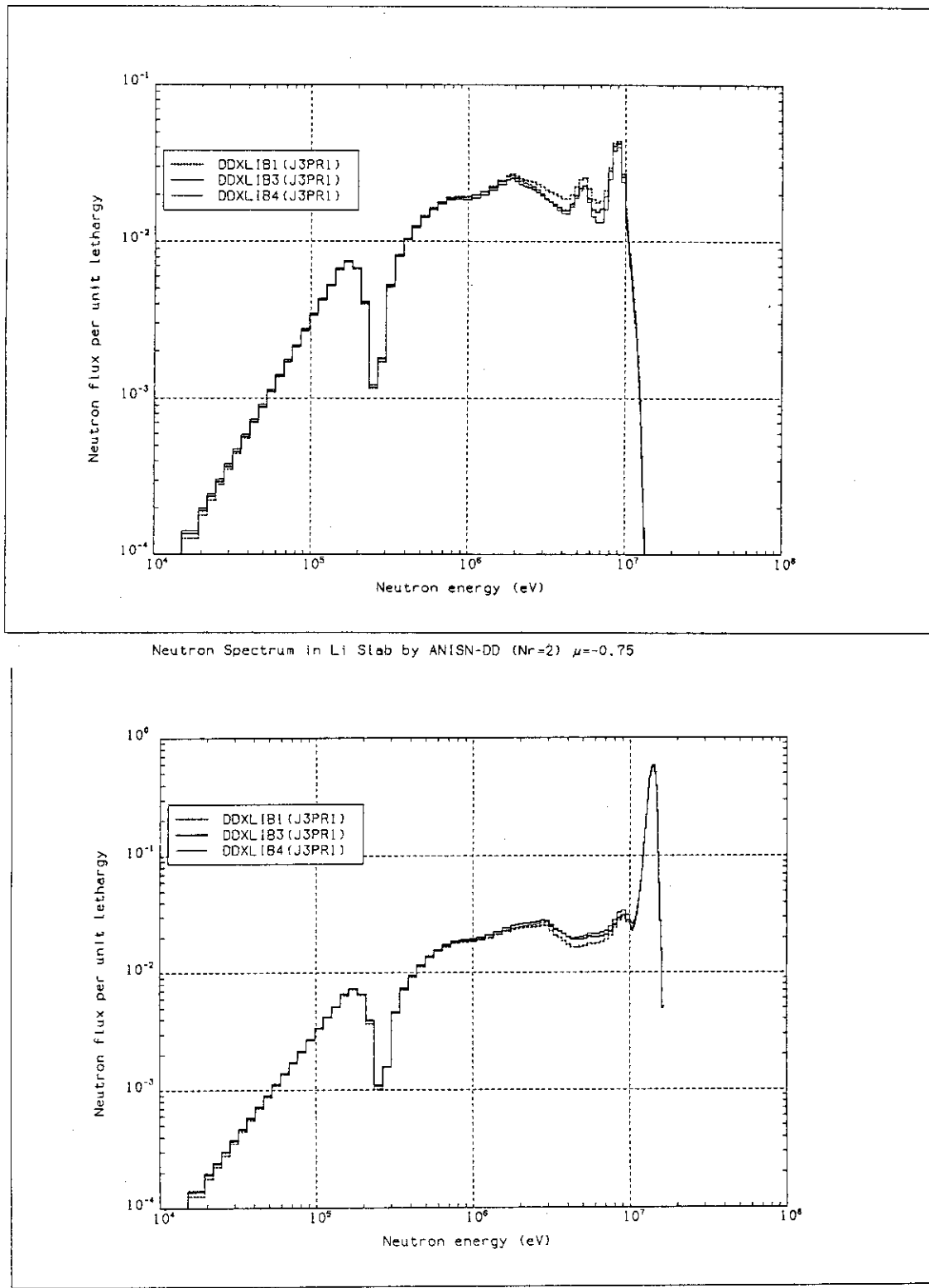
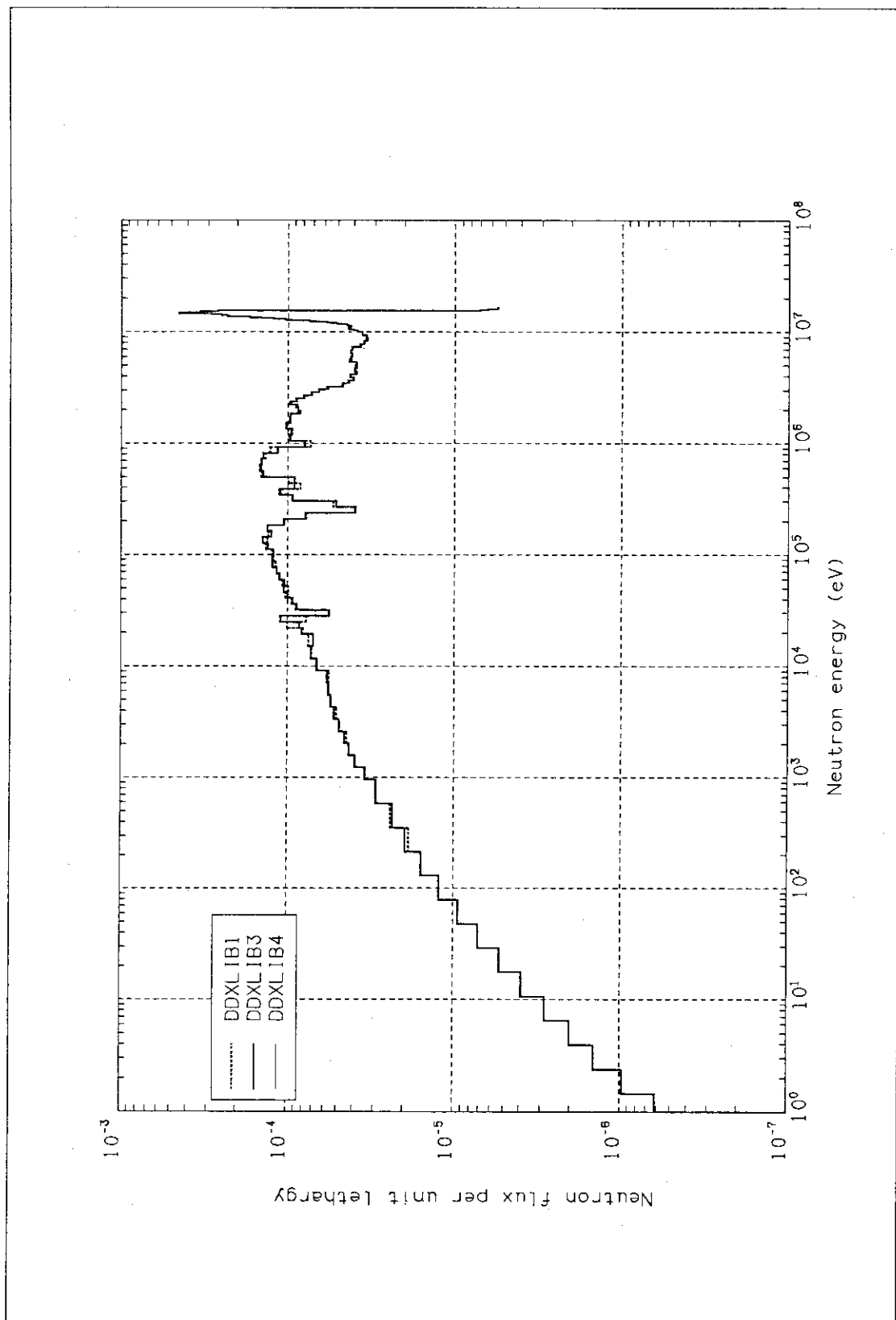


Fig.A.2 Leakage neutron spectrum from a 20 cm thick Li slab calculated with the ANISN-DD code.

Neutron Spectrum in $\text{Li}_2\text{O}-\text{C}$ by ANISN-DD ($r=20.9\text{cm}$) with JENDL-3PR1Fig A.3 Neutron spectrum in a $\text{Li}_2\text{O}-\text{C}$ sphere calculated with the ANISN-DD code.

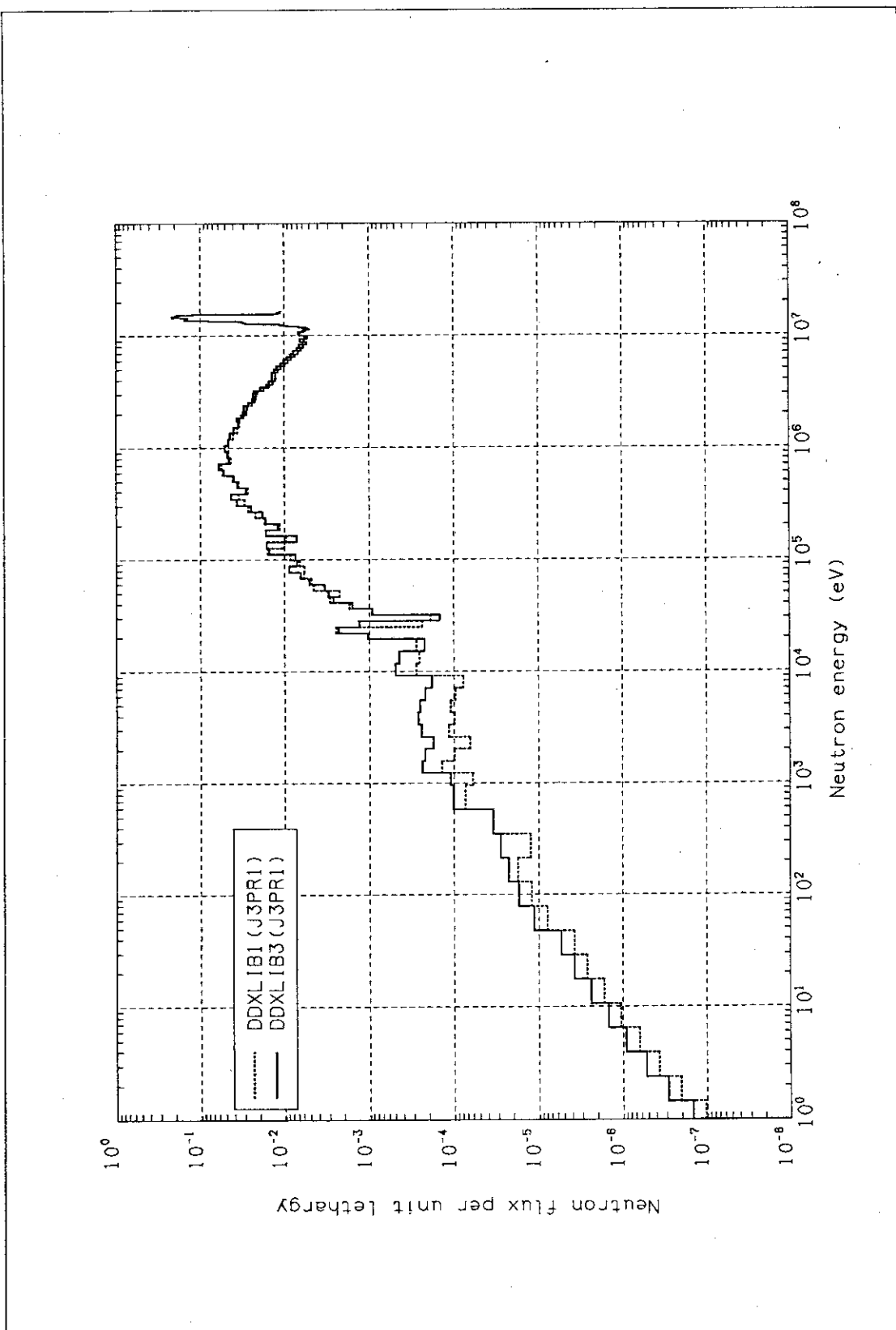
Neutron Spectrum in SUS Slab by ANISN-DD (NR=12) $\mu=0.75$

Fig.A.4 Leakage neutron spectrum from a 10 cm thick SUS slab calculated with the ANISN-DD code.